

1
2
3
4
5
6
7
8
9
10
11
12
13
14
15
16
17
18
19
20
21
22

Impact of the Vertical Mixing Induced by Low-level Jets on Boundary Layer Ozone Concentration

Xiao-Ming Hu¹, Petra M. Klein^{1,2}, Ming Xue^{1,2},
Fuqing Zhang³, David C. Doughty³, Renate Forkel⁴, Everette Joseph⁵, and Jose D. Fuentes³

¹Center for Analysis and Prediction of Storms and ²School of Meteorology,
University of Oklahoma, Norman, Oklahoma, USA

³Department of Meteorology, Pennsylvania State University, University Park, Pennsylvania,
USA

⁴Karlsruher Institut für Technologie (KIT), Institut für Meteorologie und Klimaforschung,
Atmosphärische Umweltforschung (IMK-IFU), Kreuzeckbahnstr. 19, 82467 Garmisch-
Partenkirchen, Germany

⁵Department of Physics and Astronomy, Howard University, Washington, DC, USA

1st submitted on June 5, 2012

Revision on 9/11/2012 11:10 AM

23 **Abstract**

24 After sunset, a stable boundary layer (SBL) develops close to the ground, while the upper
25 region of the daytime mixed layer becomes the residual layer (RL). Mixing between the SBL
26 and RL is often quite limited and the RL is thought to be a reservoir for daytime mixed-layer
27 pollutants under such conditions. However, ozone (O_3) profiles observed in Maryland, U.S.
28 suggest that the RL is not always a reservoir of O_3 in that region. Nocturnal low-level jets
29 (LLJs) and/or other mechanisms are speculated to enhance vertical mixing between the SBL and
30 RL, which influences the vertical O_3 redistribution.

31 Nocturnal surface O_3 maxima, a RL with reduced O_3 levels, and a concurrent strong LLJ
32 were observed in Maryland on the night of August 9-10, 2010. Surface O_3 measurements in the
33 region and three-dimensional air quality simulations suggest that horizontal advection cannot
34 explain the nocturnal O_3 maxima and concurrent decrease of O_3 levels within the RL. A
35 sensitivity study with a single column (1D) chemistry model was performed to investigate the
36 role of LLJs in generating turbulent mixing within the nighttime boundary layer and to identify
37 related impacts on O_3 concentrations at night and on the following day. The strong shear
38 associated with the LLJ enhanced turbulent mixing and weakened the decoupling of the RL and
39 SBL substantially. Ozone was actively mixed down from the RL to the surface, causing
40 secondary nocturnal surface O_3 maxima. Near the surface, O_3 was efficiently removed by
41 chemical reactions and dry deposition, which resulted in lower O_3 peak values on the next day.

43 **1. Introduction**

44 Following the traditional picture of the diurnal evolution of the atmospheric boundary layer,
45 radiational cooling after sunset results in the development of a stable boundary layer (SBL) near
46 the surface that is typically quite shallow. Above the SBL is a residual layer (RL) with
47 characteristics similar to those of the previous day's mixed layer (Stull, 1988). In the absence of
48 strong disturbances, mixing and dispersion of pollutants between the RL and SBL become
49 limited, and within the RL the concentration of pollutants remains at similar levels as in the
50 mixed layer before its decay, which is why the RL is often viewed as a reservoir of pollutants
51 (Stull, 1988). The pollutants trapped within the RL from the previous day can be entrained
52 downward into the re-developing mixed layer on the following day. In places such as the
53 northeastern United States, such downward mixing of ozone (O_3) and its precursors is shown to
54 contribute substantially to ground-level O_3 buildup in the morning in addition to chemical
55 production (Zhang et al., 1998; Zhang and Rao 1999). The downward transport of the RL O_3 in
56 the morning also contributes to the maximum O_3 levels observed near the surface during daytime
57 (Neu et al., 1994; Aneja et al., 2000; Yorks et al., 2009; Morris et al., 2010; Tong et al., 2011).
58 Accurate information regarding the RL O_3 is thus critical for correctly simulating the daytime O_3
59 near the surface (Herwehe et al., 2011). Due to its relative inaccessibility, the actual detection of
60 the properties of the RL at high temporal and spatial scales has been limited in the past. Recent
61 field experiments (e.g., Balsley et al., 2008) showed that the classical view of a quiescent RL
62 may have been oversimplified. Sporadic turbulence exists at night, weakening the decoupling
63 between the RL and SBL, and the vertical mixing in the nighttime boundary layer may be
64 significant, even compared to that in the daytime convective boundary layer (Poulos et al., 2002;
65 Tjernstrom et al., 2009). Enhanced nighttime turbulence may be triggered by mesoscale motions

66 such as low-level jets (LLJ), Kelvin-Helmholtz instabilities, gravity waves, wake vortices, and
67 density currents (Sun et al., 2002, 2003; Salmond and McKendry, 2005; Fritts et al., 2009). Such
68 intense turbulence can affect the vertical structure of the nighttime boundary layer and vertical
69 distribution of pollutants. The view of the quiescent RL as a reservoir of pollutants may be
70 challenged under such conditions. Recent observations (Hu et al., 2012) have suggested that the
71 RL is leaky at times, i.e., active vertical exchange of air exists between the RL and the SBL. As
72 a result, the O₃ levels in the RL may be highly variable and surface O₃ may not decrease as fast
73 as anticipated based on the assumption of having a completely decoupled RL and SBL. In some
74 cases, there are even secondary nighttime O₃ maxima reported, which were typically associated
75 with periods of enhanced mixing (Corsmeier et al., 1997; Reitebuch et al., 2000; Salmond and
76 McKendry, 2002; Talbot et al., 2005; Hu et al., 2012). Therefore, it is important to further
77 investigate the dynamics and mixing of nocturnal boundary layers to better understand the
78 temporal variability, absolute levels, and deposition rates of surface layer O₃ concentrations.

79 In Beltsville, Maryland (MD), nighttime vertical O₃ profiles have been measured during the
80 summertime since 2004 (Yorks et al., 2009; Hu et al., 2012). Beltsville is located between
81 Washington, D.C. and Baltimore, MD, in the middle of the Mid-Atlantic urban corridor of the
82 United States. Heavy emissions of O₃ precursors and favorable meteorological conditions
83 frequently lead to extreme O₃ events in this area (Ryan et al., 1998). Within the RL, O₃ levels at
84 the Beltsville site at times resemble those found in the free troposphere with concentrations that
85 are significantly lower than those in the previous day's atmospheric mixed layer. Ozone in the
86 RL inherited from the daytime mixed layer appears to be readily mixed down to the surface,
87 contributing to elevated O₃ at night (Hu et al., 2012). Previous studies have shown that LLJs
88 occur frequently in the Mid-Atlantic region of the United States during the period between 1900-

89 0600 hours local time (LT), with peak winds ranging from 8 to 23 m s⁻¹ (Ryan, 2004; Zhang et
90 al., 2006). Such strong LLJs may cause the RL to become leaky (Banta et al., 2007). Thus, the
91 LLJs are hypothesized to contribute to the formation of leaky RL and nighttime surface O₃
92 maxima in the Mid-Atlantic region.

93 In the current study, the impacts of a LLJ observed in the Beltsville area on surface O₃ and
94 vertical O₃ profiles are investigated in detail using different numerical modeling approaches.
95 Initially, a three-dimensional model is employed to examine the spatial extent of the LLJ and to
96 diagnose its role in modulating boundary layer O₃. A single column model is then applied to
97 isolate the impacts of the LLJ on boundary layer mixing, nocturnal O₃ dispersion, and O₃ built-
98 up on the subsequent day. This study, for the first time, provides direct modeling evidence that
99 LLJs induce substantial turbulence and reduce the RL O₃ significantly; as a result, the O₃ level in
100 the daytime boundary layer on the following day is lowered.

101

102 **2. Methods**

103 During summer 2010, a research field campaign (Hu et al., 2012) was conducted at Howard
104 University's Atmospheric Research Site in Beltsville, MD (39.06°N, 76.88°W). The
105 meteorological variables and mixing ratios of chemical species (O₃, NO, NO₂, CO, SO₂) were
106 measured at 5 m above ground level (AGL). The mixing ratios of chemical species were
107 recorded every second. During several intensive observation periods, balloon-borne
108 meteorological and O₃ sondes were used to obtain vertical profiles of temperature, humidity,
109 wind speed and direction, and O₃. On the night of August 9-10, 2010, a secondary O₃ maximum
110 and a concurrent LLJ were observed at this research site. This event will be the focus of the
111 current study. In addition to the night of August 9-10, O₃ sondes were also launched in the

112 afternoon of August 9, which provided the unique opportunity during the field campaign to
113 investigate the O₃ variation from the daytime convective boundary layer to the nighttime
114 boundary layer. LLJs commonly occur in the Mid-Atlantic region (Zhang et al., 2006). This case
115 study demonstrates potential impacts of the frequently occurring phenomenon of nocturnal LLJs
116 on boundary layer O₃.

117 Three-dimensional (3D) air quality simulations, using the Weather Research and Forecasting
118 model with Chemistry (WRF/Chem, Grell et al., 2005), for the 2010 summer campaign were
119 applied in Hu et al. (2012) to investigate regional transport of O₃ and illustrate certain caveats in
120 3D air quality simulations. As part of the current study, output from these WRF/Chem
121 simulations along with hourly O₃ data recorded at the AIRNOW sites in the region were first
122 used to examine the spatial extent and the potential causes of elevated nocturnal surface O₃
123 concentrations during the night of August 9-10, 2010. Details about the model set-up and
124 domains of the WRF/Chem simulations can be found in Hu et al. (2012).

125 To further investigate the impacts of the strong LLJ observed on the night of August 9-10,
126 2010 near the Beltsville site on the vertical distribution of O₃, a single column photochemical
127 model CACHE (Forkel et al., 2006) is employed in this study. In the vertical direction, 40 model
128 layers extend from the surface to the 2.64-km height, with a vertical grid spacing of 1 m for the
129 lowest layer and 500 m for the uppermost layer; such a setup appears to adequately capture the
130 boundary layer structure during both nighttime and daytime. The multi-layered photochemical
131 model solves the following system of equations:

$$132 \quad \frac{\partial x_{i,j}}{\partial t} = E_{i,j} + D_{i,j} + C_{i,j} + \frac{\partial}{\partial z} \left(K \frac{\partial x_{i,j}}{\partial z_j} \right) \quad (1)$$

133 where subscripts i and j denote the i^{th} chemical species and the j^{th} model layer, respectively, with

134 χ being the concentration of a chemical species. Terms E , D and C are the rates of change due
135 to emissions, dry deposition, and chemical reactions, respectively. The estimation method of
136 emissions of volatile organic compounds, E , was updated to use the formula of Guenther (2006).
137 The dry deposition, D , is treated using the methods of Wesely (1989) and Gao et al. (1993). The
138 chemical reaction rate, C , is computed using the Regional Atmospheric Chemistry Mechanism
139 (RACM) gas-phase mechanism (Stockwell et al., 1997). The atmospheric turbulent transport
140 term, i.e., the last term of (1), is parameterized using a first-order closure scheme. The eddy
141 diffusivity K is described using a mixing-length approach, in which K is expressed as a function
142 of mixing length l , the vertical wind shear S , and the stability function $f(Ri)$:

$$143 \quad K = l^2 S f(Ri) \quad (2)$$

144 This first-order parameterization is widely applied in operational NWP and climate models
145 (Beare et al., 2006; Cuxart et al., 2006). The stability function f is parameterized using the
146 Richardson number Ri ; a larger/smaller Ri leads to a smaller/larger value of the stability function.
147 The Richardson number Ri , a dynamic stability parameter, represents the ratio of thermally to
148 mechanically produced turbulence in a defined air layer.

149 Two simulations are conducted with the single column model. In the control simulation,
150 a calm condition (no LLJ) is considered while in a sensitivity simulation a LLJ is included. The
151 simulations are initialized at 1400 LT on August 9, 2010, and run for 34 hours. The initial
152 concentrations of O_3 and nitrogen oxides (NO_x) come from field observations while the initial
153 concentrations of other species come from the WRF/Chem simulation conducted in Hu et al.
154 (2012). The shortwave radiation is constrained by the observed values. The simulated mixing
155 ratio of NO_x in the boundary layer is nudged to the observed values at 5m AGL every half-hour.
156 Advection is not considered in the single column model. The boundary layer advection pathway

157 in Maryland changed during the daytime of August 10, 2010 (Hu et al., 2012). Thus bias of the
158 simulated mixed layer O₃ on August 10 by the single column model is expected. However, the
159 goal of the single column model simulations is to isolate the impact of the vertical mixing
160 induced by a LLJ on boundary layer O₃ by examining the difference between the control and the
161 sensitivity simulations.

162 **3. Observations and three-dimensional WRF/Chem simulations**

164 The measured O₃, NO_x and the corresponding meteorological variables on August 9-10,
165 2010 at the Beltsville research site, 5 m AGL, are shown in Fig. 1. Due to the diurnal cycle of
166 photochemical production, O₃ maxima typically occur in the afternoon in the continental
167 atmospheric boundary layer. During summer nights, NO_x mixing ratios are ~7 ppbv and NO
168 titration and dry deposition usually result in continuously decreasing O₃ concentrations near the
169 surface in Beltsville (Hu et al., 2012). During our study period, however, a secondary O₃
170 maximum was recorded on the night of August 9-10, 2010; O₃ mixing ratios between 0000 and
171 0300 LT were elevated by ~15 ppbv. By 0700 and 0800 LT, the O₃ mixing ratio decreased to
172 ~10 ppbv due to NO titration and dry deposition. The secondary O₃ maximum was accompanied
173 by a decrease of the NO_x mixing ratio and increase of temperature. Southwesterly winds (~2 m
174 s⁻¹) were maintained during the period of 0000-0500 LT, suggesting that a similar footprint and
175 air mass persisted during this period. These factors suggest that the secondary O₃ maximum at
176 the surface on the night of August 9-10, 2010 was due to downward mixing of RL O₃, as was
177 also reported in Talbot et al. (2005) and Hu et al. (2012). Since the upper layers typically had
178 higher O₃ mixing ratios, lower NO_x mixing ratios, and higher potential temperatures, one can
179 conclude that vertical mixing between the SBL and RL persisted during the night, which led to

180 an increase in surface O₃ and temperature, and a decrease in surface NO_x.

181 Similar secondary nocturnal O₃ maxima were also recorded at the majority of AIRNOW
182 sites (60% of 45 sites) along the Virginia-to-Connecticut corridor on the same night. Other
183 AIRNOW sites along this corridor also experienced elevated O₃ on this night, but an isolated
184 secondary O₃ maximum was not apparent. The concentration variations for ten exemplary sites
185 are shown in Fig. 2. Figure 3 illustrates the locations of those sites. These AIRNOW sites are
186 located across a wide region with different characteristics such as urban and rural land use types.
187 Their upstream O₃ mixing ratios varied significantly according to the WRF/Chem simulation
188 (Fig. 4), which can be explained by the different elevation of the monitoring sites (Fig. 3) and
189 spatially variable precursor emission rates within the domain. Ozone was removed more
190 efficiently by NO titration around anthropogenic emission sources such as big cities and traffic
191 roads. Factors contributing to higher nighttime O₃ concentrations at elevated locations (e.g., in
192 the Appalachian Mountains) included (1) a more explicit influence of O₃-richer air from the free
193 troposphere, (2) lower anthropogenic emission rates, and (3) limited transport of NO into these
194 regions. Despite the heterogeneous upstream O₃ mixing ratios, almost concurrent nocturnal
195 secondary O₃ maxima were observed at the AIRNOW sites along the Virginia-to-Connecticut
196 corridor. Given the large variability in O₃ concentrations near each site, advection cannot
197 explain these nearly simultaneous secondary maxima. The distance between the south-west (S.
198 MARYND) and north-east (Mt Ninham) sites along the corridor is ~600 km. Even with a wind
199 speed as high as 20 m s⁻¹, it would take more than eight hours for an air mass to travel across this
200 distance. The secondary O₃ maximum at Mt Ninham would be expected to occur several hours
201 later than at the S. MARYND site if they were due to advection of an O₃-richer air mass, which
202 was clearly not observed. Given the difficulties in reproducing the structure of the nocturnal

203 boundary layer and nighttime chemistry, the simulated vertical profile of chemical species can be
204 biased (Zhang et al., 2009; Herwehe et al., 2011; Hu et al., 2012). Thus, the results from the
205 WRF/Chem simulations should not be over interpreted. It can be noted, however, that the
206 general O₃ patterns remain similar throughout the entire period from 0000 LT to 0400 LT
207 (Figure not shown), which is another indication that advection did not play a crucial role in the
208 formation of the nighttime secondary O₃ maxima. The small variations in the onset times of the
209 secondary O₃ maxima among the ten sites (Fig. 2) do not show any systematic trends related to
210 the position of the site along the SW-NE corridor. They can likely be explained by the local
211 characteristics of each site (e.g., urban vs. rural and different elevation), which resulted in
212 different nocturnal O₃-depletion rates, vertical O₃ distributions, and turbulent mixing at each site.

213 Boundary layer structures on August 9-10, 2010 are clearly illustrated by the measured
214 vertical profiles of O₃ (Fig. 5a). During daytime, elevated O₃ mixing ratios due to photochemical
215 production are confined in the mixed layer, which is the lower ~1.7 km AGL. The O₃ mixing
216 ratio in the daytime mixed layer on August 9, 2010 was as high as 100 ppbv (Fig. 5a). During
217 nighttime, strong vertical gradients of O₃ mixing ratios develop in the stable boundary layer (~
218 600 m AGL) due to efficient O₃ removal by NO titration and dry deposition near the surface. If
219 the stable boundary layer developing near the surface is decoupled from the RL, we would
220 expect to observe low O₃ concentrations close to the surface, but concentrations inside the RL
221 would remain close to the values observed within the previous day mixed layer (~100 ppbv in
222 the studied case). However, O₃ concentrations decreased throughout the RL (0.8-1.7 km AGL)
223 on the night of August 9-10, 2010 to as low as 50-60 ppbv, which more closely resemble the
224 values in the free troposphere. The decrease of the RL O₃ concentrations by nearly a factor of 2
225 compared to the previous day mixed-layer values, confirms that active dispersion of RL O₃

226 persisted on this night. At the same time, a strong LLJ over the Beltsville research site was
227 recorded during the study period. The wind speed exceeded 15 m s^{-1} at 500 m AGL at 0252 LT
228 on August 10 (Fig. 5b). Along the western, mountainous side of the Virginia-to-Connecticut
229 corridor, strong radiative cooling near the ground results in lower nighttime temperatures than on
230 the eastern side. Such a horizontal temperature gradient, caused by the terrain effects (Fig. 3),
231 can induce a southwesterly thermal wind in the nocturnal boundary layer (Ryan, 2004), and
232 contribute to the formation of the nighttime LLJ. The meridional variation of the Coriolis
233 parameter could also accelerate the northward-blowing LLJ (Wexler, 1961; Zhong et al., 1996).
234 The results from WRF/Chem simulations reported in Hu et al. (2012) also showed that a
235 persistent low-level jet formed east of the Appalachian Mountains over the Virginia-to-
236 Connecticut corridor (Fig. 6). Compared with the observed wind profiles, the maximum LLJ
237 wind speed was however significantly underestimated by WRF (Fig. 7). Beltsville and all the
238 sites experiencing secondary O_3 maximum shown in Fig. 2 are located in the corridor affected by
239 the LLJ. As it was already discussed, neither the observations nor the model results indicate that
240 advection of O_3 triggered the secondary, nighttime O_3 maxima. Instead, it is hypothesized that
241 the LLJ induced strong turbulence, which weakened the decoupling between the SBL and RL
242 and triggered enhanced mixing of O_3 from the RL to the ground, causing the observed increase in
243 surface O_3 . To prove this hypothesis, a one-dimensional modeling study was conducted that
244 allowed us to isolate the role of the LLJ.

245

246 **4. Impact of LLJ-induced vertical mixing in one-dimensional simulations**

247 The 3D WRF/Chem simulation predicted that a LLJ formed and persisted throughout the
248 early morning hours. However, it significantly underestimated the strength of the LLJ (Fig. 7),

249 which meant that the WRF/Chem model would not accurately reproduce the vertical mixing in
250 the NBL. However, even if the simulation had correctly reproduced the LLJ strength, it would
251 still be difficult to identify the contribution of the LLJ in moderating the vertical O₃ distribution
252 because the interplay of several processes (e.g., vertical mixing and horizontal advection) cannot
253 be easily separated in 3D simulations. Therefore, simulations are conducted in this study using a
254 single-column model to examine the impact of LLJ-induced vertical mixing on August 10, 2010.
255 The environmental wind profile is manually set up in the model using the observed wind profile
256 as guidance. Two simulations are conducted; the control simulation has a calm condition while a
257 sensitivity experiment has a LLJ profile between 0000 LT and 0600 LT of day 2; the latter is
258 otherwise the same as the control simulation. The maximum wind speed (WSP) of the LLJ at
259 440 m AGL is set as 20 m s⁻¹. The single column model does not consider directional wind
260 shear. Instead, the maximum WSP of the LLJ is set at a higher value than the observation to
261 account for the effect of directional shear-induced turbulence.

262 The simulations with the single column model captured the meteorological conditions (e.g.,
263 temperature and relative humidity) reasonably well (Fig. 8). In the sensitivity simulation, the
264 impacts of LLJ-induced vertical mixing on meteorological conditions near the surface are
265 successfully captured. An abrupt increase of temperature and decrease of relative humidity near
266 the surface are reproduced at the onset of the LLJ, i.e., 0000 LT on August 10, 2010.

267 The simulated time series of O₃ mixing ratios near the surface are shown in Fig. 9a. At the
268 onset of the LLJ (0000 LT), O₃ mixing ratios near the surface increased by ~18 ppbv in the
269 sensitivity simulation. At the same time, surface temperature increased (Fig. 8). These results
270 are consistent with the observed secondary O₃ maximum shown in Fig. 1. The surface O₃ was
271 nearly depleted on the calm night in the control simulation due to dry deposition and NO titration,

272 while it was elevated in the sensitivity simulation with the LLJ (Fig. 9a). Such difference of the
273 surface O₃ caused by LLJs was also reported in previous studies (Banta et al., 2007). These
274 results therefore confirm the hypothesis that the LLJ played an important role in downward
275 mixing of O₃ during the night of August 9-10, 2010.

276 The simulated vertical profiles of O₃ are shown in Fig. 10. The LLJ played an important role
277 in removing O₃ in the RL at night. According to the formula (2), elevated wind shear in the
278 presence of the LLJ will cause an increase of the eddy diffusivity. As a result of the shear-
279 enhanced turbulence, the temperature inversion weakened, *Ri* further decreased, which,
280 according to (2), as a whole contributed to a substantial increase in eddy diffusivity in the
281 presence of a LLJ. The enhanced vertical mixing played a critical role in modulating the vertical
282 redistribution of O₃ in the boundary layer. On a calm night, O₃ in the RL was mostly conserved
283 while the RL O₃ was reduced by ~25 ppbv at 0800 LT in the presence of the LLJ (Fig. 10 and
284 Fig. 9b). LLJs have also been reported to induce mechanical turbulence that can vertically mix
285 O₃ in the nocturnal boundary layer in other regions such as Texas (Tucker et al., 2010). The
286 significant reduction of O₃ in the RL in both observations (Fig. 5a) and simulation (Fig. 10b)
287 indicates that the RL may not be a reservoir of pollutants in the presence of strong LLJs. The
288 simulated reduction of the RL O₃ from the daytime mixed layer by the sensitivity simulation
289 (~25 ppbv, Fig. 10b) was smaller than the observed reduction (~40 ppbv, Fig. 5a). Such
290 discrepancy may be due to the exclusion of advection processes in the single column model
291 and/or model errors. Model errors in the treatments of vertical mixing in meteorological and air
292 quality models are shown to lead to substantial bias of simulated profiles of meteorological and
293 chemical variables (Hu et al., 2010, 2012; Nielsen-Gammon et al., 2010).

294 Due to the enhanced turbulence induced by the LLJ, more O₃ was transported to the surface,
295 where it was subjected to NO titration and enhanced dry deposition. The dry deposition velocity
296 was correlated to the friction velocity u_* , with larger u_* values leading to larger dry deposition
297 velocities. Enhanced turbulent mixing in the presence of a LLJ resulted in an increase in u_* , and
298 thus higher dry deposition rates. As a result, the LLJ affected the O₃ budget at night, which in
299 turn affected the O₃ concentration in the daytime mixed layer on the following day. Figure 10
300 shows that the mixed-layer O₃ at 1400 LT on the second day was reduced by ~8 ppbv due to the
301 influence of the LLJ compared to the control simulation without the LLJ. The simulated
302 maximum surface O₃ on August 10, 2010 was reduced by ~8 ppbv with the LLJ while the
303 maximum 8-hour running average O₃ was reduced by ~6 ppbv (Fig. 9a). Compared with the
304 observed O₃ profile at 13:54 LT on August 10 (~80 ppbv in the mixed layer), the predicted O₃ in
305 the mixed layer on the second day by the sensitivity simulation is higher by ~10 ppbv. The
306 discrepancy is likely due to the change of transport pathways during the daytime of August 10,
307 2010 (Hu et al., 2012), which is not considered in the single column model.

308 The time-height diagrams of simulated O₃ are shown in Fig. 11. Without the LLJ, the RL O₃
309 is mostly conserved (Fig. 11a). When the daytime mixed layer grows, the O₃-rich RL air is
310 entrained into the mixed layer below, thereby contributing to the rapid increase in O₃ in the
311 mixed layer in the morning. Such a scenario is described in Zhang and Rao (1999) and
312 confirmed by other studies (Aneja et al., 2000; Yorks et al., 2009; Morris et al., 2010; Tong et
313 al., 2011). However, in the presence of the LLJ, the RL O₃ is removed at night (Fig. 11b). In the
314 following morning, entrainment contributes much less to the O₃ in the mixed layer (Fig. 11b),
315 thus the increase of surface O₃ is much slower comparing to the control simulation (Fig. 9a).

316

317 **5. Conclusions and discussion**

318 Profiles of O₃ and meteorological variables in both nighttime and daytime have been
319 measured in summertime since 2006 in Beltsville, Maryland (Hu et al., 2012). The data sets
320 provided a unique opportunity to investigate the pollutants in the residual layer (RL) and their
321 contribution to the daytime boundary layer pollution. It is shown that the RL was at times not a
322 reservoir of O₃ at night. A case study was conducted for August 9-10, 2010, when a strong LLJ
323 and elevated surface O₃ were observed at night. During this night, the RL O₃ was 50-60 ppbv,
324 which was much lower than the O₃ level in the mixed layer on the previous day (~100 ppbv).
325 Thus, O₃ appeared to be mixed from the RL to the ground preventing the RL from acting like a
326 reservoir. Simulation results from a single-column model containing O₃ chemistry confirm that
327 the LLJ causes a nocturnal secondary O₃ maximum and a significant reduction of the RL O₃.
328 The LLJ-induced strong turbulence, which transports O₃-rich RL air to the surface where O₃ is
329 efficiently removed by chemical reactions and enhanced dry deposition. These processes impact
330 the O₃ budget: the enhanced nocturnal vertical mixing reduces the increase in surface O₃ the
331 following morning and, compared to the results of a control simulation with calm conditions, the
332 maximum O₃ is ~ 8 ppbv lower for the simulation containing a LLJ.

333 Salmond and McKendry (2002) found that secondary surface O₃ maximum due to enhanced
334 nocturnal mixing rarely exceeded 50 ppbv. They concluded that the nocturnal secondary O₃
335 maximum is unlikely to be significant enough to affect human health. Our study shows that such
336 nocturnal mixing may play an important role in modulating the O₃ levels in the daytime
337 boundary layer on the following day; it may thus have a more important implication for public
338 health than it had been previously realized.

339 Ryan (2004) investigated the climatology of LLJs in Maryland, USA and found that the
340 weather patterns favorable for the development of LLJs are normally also suitable for the
341 occurrence of Mid-Atlantic high O₃ episodes. Thus, the influence of LLJs on the O₃ episodes
342 can be hardly discerned from other factors that are conducive to O₃ accumulation. Due to the
343 difficulty in accurately reproducing LLJs and the interplay of several processes (e.g., vertical
344 mixing and horizontal advection) in three dimensional air quality simulations, a previous study
345 on this case (Hu et al. 2012) did not isolate the impact of LLJs on the vertical distribution of O₃.
346 Using a single column chemistry model that allows for easier setup of sensitivity experiments in
347 this study, the impact of LLJs on the boundary layer O₃ pertaining to stronger vertical mixing is
348 isolated. The effects of horizontal long-range transport due to LLJs are not considered in this
349 study. One implication of this study for long-range transport is: the pollutants in the RL may
350 leak out during the horizontal transport due to enhanced vertical mixing, reducing the impact of
351 urban plumes in downwind areas.

352 LLJs have been reported in many regions (Whiteman et al., 1997; Song et al., 2005; Zhang et
353 al., 2006); the LLJs in other regions (e.g., the Great Plains of the United States) may be much
354 stronger and more extensive than those in the Mid-Atlantic region (Zhang et al., 2006). Thus,
355 the impact of LLJs on the boundary layer O₃ may have important implications for air quality in
356 many regions. Apart from LLJs, mesoscale motions such as Kelvin-Helmholtz instabilities,
357 gravity waves, wake vortices, and density currents can also cause enhanced nighttime turbulence
358 (Sun et al., 2002, 2003; Salmond and McKendry, 2005; Fritts et al., 2009), which may also make
359 the RL leaky. In addition to O₃, nocturnal mixing events may have appreciable effects on the
360 dispersion and budget of other species such as carbon dioxide and volatile organic compounds
361 (Acevedo et al., 2006; Ganzeveld et al., 2008). In one-dimensional simulations for the boundary

362 layer over a tropical forest using a single column chemistry-climate model, Ganzeveld et al.
363 (2008) showed that unresolved nocturnal vertical mixing processes likely lead to a nocturnal
364 accumulation of formaldehyde in the RL, which is later on entrained into the daytime convective
365 boundary layer where it affects daytime photochemistry. Further investigations regarding such
366 mixing processes and their impacts are warranted. Future field campaigns that aim at improving
367 our understanding of atmospheric chemistry in the atmospheric boundary layer should include
368 measurements of the chemical composition/transformation in combination with detailed
369 measurements of turbulence inside the RL.

370 Although the current study focuses on demonstrating the importance of vertical mixing
371 processes for vertical dispersion of boundary layer O₃, the contribution of other processes,
372 including advection (Banta et al., 2005; Zhang et al. 2007; Tucker et al., 2010), dry deposition
373 (Lin and McElroy, 2010) and chemical reactions in different chemical regimes at different height
374 above the ground (Brown et al., 2007), cannot be always ignored. To more accurately quantify
375 their contributions, meteorological and air chemistry measurements throughout the atmospheric
376 boundary layer are needed to further improve boundary-layer parameterizations, particularly for
377 nighttime conditions, and to facilitate the development and evaluation of more sophisticated
378 three-dimensional chemistry simulations.

379
380 *Acknowledgement.* This work was supported by funding from the Office of the Vice President
381 for Research at the University of Oklahoma. The second author was also supported through the
382 NSF Career award ILREUM (NSF ATM 0547882). DCD received support from NASA (grant
383 number NNX08BA42A) to participate in the field studies. JDF received support from the
384 National Science Foundation to participate in this research (award ATM 0914597).

385 *Observations at Howard University Beltsville Campus were supported through grants from*
386 *Maryland Department of the Environment, NASA (grant number NNX08BA42A) and NOAA*
387 *(grant number NA17AE1625).*

388 **References**

389 Acevedo, O. C., Moraes, O. L. L., Degrazia, G. A., Medeiros, L. E., 2006. Intermittency and the
390 exchange of scalars in the nocturnal surface layer. *Boundary-Layer Meteorology* 119, 41–55.

391 Aneja, V. P., Mathur, R., Arya, S. P., Li, Y., Murray, G. C., Manuszak, T. L., 2000. Coupling the
392 vertical distribution of ozone in the atmospheric boundary layer. *Environmental Science &*
393 *Technology* 34, 2324–2329.

394 Balsley, B., Svensson, G., Tjernström, M., 2008. On the scale dependence of the gradient
395 Richardson number in the residual layer. *Boundary-Layer Meteorology* 127, 57–72.

396 Banta, R. M., Seniff, C. J., Nielsen-Gammon, J., Darby, L. S., Ryerson, T. B., Alvarez, R. J.,
397 Sandberg, S. P., Williams, E. J., Trainer, M., 2005. A Bad Air Day in Houston. *Bulletin of*
398 *American Meteorological Society* 86, 657-669.

399 Banta, R. M., Mahrt, L., Vickers, D., Sun, J., Balsley, B. B., Pichugina, Y. L., Williams, E. J.,
400 2007. The Very Stable Boundary Layer on Nights with Weak Low-Level Jets. *Journal of the*
401 *Atmospheric Sciences* 64, 3068–3090.

402 Beare, R. J., et al., 2006. An intercomparison of large-eddy simulations of the stable boundary
403 layer. *Boundary-Layer Meteorology* 118(2), 247–272.

404 Brown, S.S., Dube, W.P., Osthoff, H.D., Wolfe, D.E., Angevine, W.M., Ravishankara, A.R.,
405 2007. High resolution vertical distributions of NO₃ and N₂O₅ through the nocturnal boundary
406 layer. *Atmospheric Chemistry and Physics* 7, 139–149.

407 Corsmeier, U., Kalthoff, N., Kolle, O., Kotzian, M., Fiedler F., 1997. Ozone concentration jump
408 in the stable nocturnal boundary layer during a LLJ-event. *Atmospheric Environment* 31,
409 1977-1989.

410 Cuxart, J., et al., 2006. Single-column model intercomparison for a stably stratified atmospheric
411 boundary layer. *Boundary-Layer Meteorology* 118, 273–303.

412 Forkel, R., Klemm, O., Graus, M., Rappengluck, B., Stockwell, W. R., Grabmer, W., Held, A.,
413 Hansel, A., Steinbrecher, R., 2006. Trace gas exchange and gas phase chemistry in a Norway
414 spruce forest: A study with a coupled 1-dimensional canopy atmospheric chemistry emission
415 model. *Atmospheric Environment* 40, 28–42.

416 Fritts, D. C., Wang, L., Werne, J., 2009. Gravity wave–fine structure interactions: A reservoir of
417 small-scale and large-scale turbulence energy. *Geophysical Research Letters* 36, L19805,
418 doi:10.1029/2009GL039501.

419 Gao, W., Wesely, M. L., Doskey, P. V., 1993. Numerical Modeling of the Turbulent Diffusion
420 and Chemistry of NO_x, O₃, Isoprene, and Other Reactive Trace Gases in and Above a Forest
421 Canopy. *Journal of Geophysical Research* 98(D10), 18,339–18,353, doi:10.1029/93JD01862.

422 Ganzeveld, L., et al., 2008. Surface and boundary layer exchanges of volatile organic compounds,
423 nitrogen oxides and ozone during the GABRIEL campaign. *Atmospheric Chemistry and*
424 *Physics* 8, 6223–6243.

425 Guenther, A., Karl, T., Harley, P., Wiedinmyer, C., Palmer, P. I., Geron, C., 2006. Estimates of
426 global terrestrial isoprene emissions using MEGAN. *Atmospheric Chemistry and Physics* 6,
427 3181-3210.

428 Grell, G. A., Peckham, S. E., Schmitz, R., McKeen, S. A., Frost, G., Skamarock, W. C., Eder, B.,
429 2005. Fully coupled online chemistry within the WRF model. *Atmospheric Environment* 39,
430 6957–6975.

431 Herwehe, J. A., Otte, T. L., Mathur, R., Rao, S. T., 2011. Diagnostic analysis of ozone
432 concentrations simulated by two regional-scale air quality models. *Atmospheric Environment*
433 45(33), 5957-5969

434 Hu, X.-M., Nielsen-Gammon, J. W., Zhang, F., 2010. Evaluation of Three Planetary Boundary
435 Layer Schemes in the WRF Model. *Journal of Applied Meteorology and Climatology* 49,
436 1831–1844.

437 Hu, X.-M., et al., 2012. Ozone variability in the atmospheric boundary layer in Maryland and its
438 implications for vertical transport model. *Atmospheric Environment* 46, 354-364.

439 Lin, J. T., McElroy, M. B., 2010. Impacts of boundary layer mixing on pollutant vertical profiles
440 in the lower troposphere: Implications to satellite remote sensing. *Atmospheric Environment*
441 44 (14), 1726–1739.

442 Morris, G. A., Ford, B., Rappengluck, B., Thompson, A. M., Mefferd, A., Ngan, F., Lefer, B.,
443 2010. An evaluation of the interaction of morning residual layer and afternoon mixed layer
444 ozone in Houston using ozonesonde data. *Atmospheric Environment* 44, 4024-4034.

445 Neu, U., Kunzle, T., Wanner, H., 1994. On the relation between ozone storage in the residual
446 layer and the daily variation in near surface ozone concentration-A case study. *Boundary-
447 Layer Meteorology* 69, 221-247.

448 Nielsen-Gammon, J.W., Hu, X.-M., Zhang, F., Pleim, J.E., 2010. Evaluation of planetary
449 boundary layer scheme sensitivities for the purpose of parameter estimation. *Monthly
450 Weather Review* 138, 3400-3417.

451 Noh, Y., Cheon, W. G., Hong, S-Y., Raasch, S., 2003. Improvement of the K-profile model for
452 the planetary boundary layer based on large eddy simulation data. *Boundary-Layer
453 Meteorology* 107, 401–427.

454 Poulos, G. S., et al., 2002. CASES-99: A Comprehensive Investigation of the Stable Nocturnal
455 Boundary Layer. *Bulletin of American Meteorological Society* 83, 555–581.

456 Reitebuch, O., Strassburger, A., Emeis, S., Kuttler, W., 2000. Nocturnal secondary ozone
457 concentration maxima analysed by sodar observations and surface measurements.
458 *Atmospheric Environment* 34, 4315-4329.

459 Ryan, W. F., et al., 1998. Pollutant transport during a regional O₃ episode in the Mid-Atlantic
460 states. *Journal of the Air & Waste Management Association* 48, 786–797.

461 Ryan, W. F., 2004. The low-level jet in Maryland: profiler observations and preliminary
462 climatology. A report prepared for the Maryland Department of the Environment.

463 Salmond, J.A., McKendry, I.G., 2002. Secondary ozone maxima in a very stable nocturnal
464 boundary layer: observations from the Lower Fraser Valley, B.C. *Atmospheric Environment*
465 36, 5771–5782.

466 Salmond, J. A., McKendry, I. G., 2005. A review of turbulence in the very stable boundary layer
467 and its implications for air quality. *Progress in Physical Geography* 29, 171–188.

468 Song, J., Liao, K., Coulter, R. L., Lesht, B. M., 2005. Climatology of the Low-Level Jet at the
469 Southern Great Plains Atmospheric Boundary Layer Experiments Site. *Journal of Applied*
470 *Meteorology* 44, 1593–1606.

471 Stockwell, W. R., Kirchner, F., Kuhn, M., Seefeld, S., 1997. A new mechanism for regional
472 atmospheric chemistry modeling. *Journal of Geophysical Research* 102, 25 847–25 879.

473 Sun, J., et al., 2002. Intermittent turbulence associated with a density current passage in the
474 stable boundary layer. *Boundary-Layer Meteorology* 105, 199–219.

475 Sun, J., et al., 2003. Atmospheric disturbances that generate intermittent turbulence in nocturnal
476 boundary layers. *Boundary-Layer Meteorology* 110, 255–279.

477 Stull, R. B., 1988. *An Introduction to Boundary Layer Meteorology*, Kluwer, Norwell, Mass.

478 Talbot, R., Mao, H., Sive, B., 2005. Diurnal characteristics of surface level O₃ and other
479 important trace gases in New England. *Journal of Geophysical Research* 110, D09307,
480 doi:10.1029/2004JD005449.

481 Tjernström, M., Balsley, B. B., Svensson, G., Nappo, C. J., 2009. The Effects of Critical Layers
482 on Residual Layer Turbulence. *Journal of the Atmospheric Sciences* 66, 468–480.

483 Tong, N.Y.O., Leung, D.Y.C., Liu, C.H., 2011. A review on ozone evolution and its relationship
484 with boundary layer characteristics in urban environments. *Water, Air, & Soil Pollution* 214,
485 13-36.

486 Tucker, S. C., et al., 2010. Relationships of coastal nocturnal boundary layer winds and
487 turbulence to Houston ozone concentrations during TexAQS 2006. *Journal of Geophysical*
488 *Research* 115, D10304, doi:10.1029/2009JD013169.

489 Wesely, M. L., 1989. Parameterization of surface resistances to gaseous dry deposition in region-
490 scale numerical models. *Atmospheric Environment* 23, 1293–1304.

491 Wexler, H., 1961. A boundary layer interpretation of the low-level jet. *Tellus*, 13, 368–378.

492 Whiteman, C. D., Bian, X., Zhong, S., 1997. Low-Level Jet Climatology from Enhanced
493 Rawinsonde Observations at a Site in the Southern Great Plains. *Journal of Applied*
494 *Meteorology* 36, 1363–1376.

495 Yorks, J.E., Thompson, A. M., Joseph, E., Miller, S. K., 2009. The Variability of Free
496 Tropospheric Ozone over Beltsville, Maryland (39N, 77W) in the Summers 2004-2007.
497 *Atmospheric Environment* 43, 1827-1838.

498 Zhang, D.-L., Zhang, S., Weaver, S. J., 2006. Low-Level Jets over the Mid-Atlantic States:
499 Warm-Season Climatology and a Case Study. *Journal of Applied Meteorology and*
500 *Climatology* 45, 194–209.

501 Zhang, F., Bei, N., Nielsen-Gammon, J. W., Li, G., Zhang, R., Stuart, A. L., Aksoy, A., 2007.
502 Impacts of meteorological uncertainties on ozone pollution predictability estimated through
503 meteorological and photochemical ensemble forecasts. *Journal of Geophysical*
504 *Research* 230, D04304, doi:10.1029/2006JD007429.

505 Zhang, J., Rao, S. T., 1999. The role of vertical mixing in the temporal evolution of ground-level
506 ozone concentrations. *Journal of Applied Meteorology* 38, 1674 – 1691.

507 Zhang, J., Rao, S. T., Daggupati, S. M., 1998. Meteorological Processes and Ozone
508 Exceedances in the Northeastern United States during the 12–16 July 1995 Episode. *Journal*
509 *of Applied Meteorology*, 37, 776–789.

510 Zhang, Y., Dubey, M. K., Olsen, S. C., Zheng, J., Zhang, R., 2009. Comparisons of WRF/Chem
511 simulations in Mexico City with ground-based RAMA measurements during the 2006-
512 MILAGRO. *Atmospheric Chemistry and Physics*, 9, 3777–3798.

513 Zhong, S., Fast, J. D., Bian, X., 1996. A Case Study of the Great Plains Low-Level Jet Using
514 Wind Profiler Network Data and a High-Resolution Mesoscale Model. *Monthly Weather*
515 *Review* 124, 785–806.

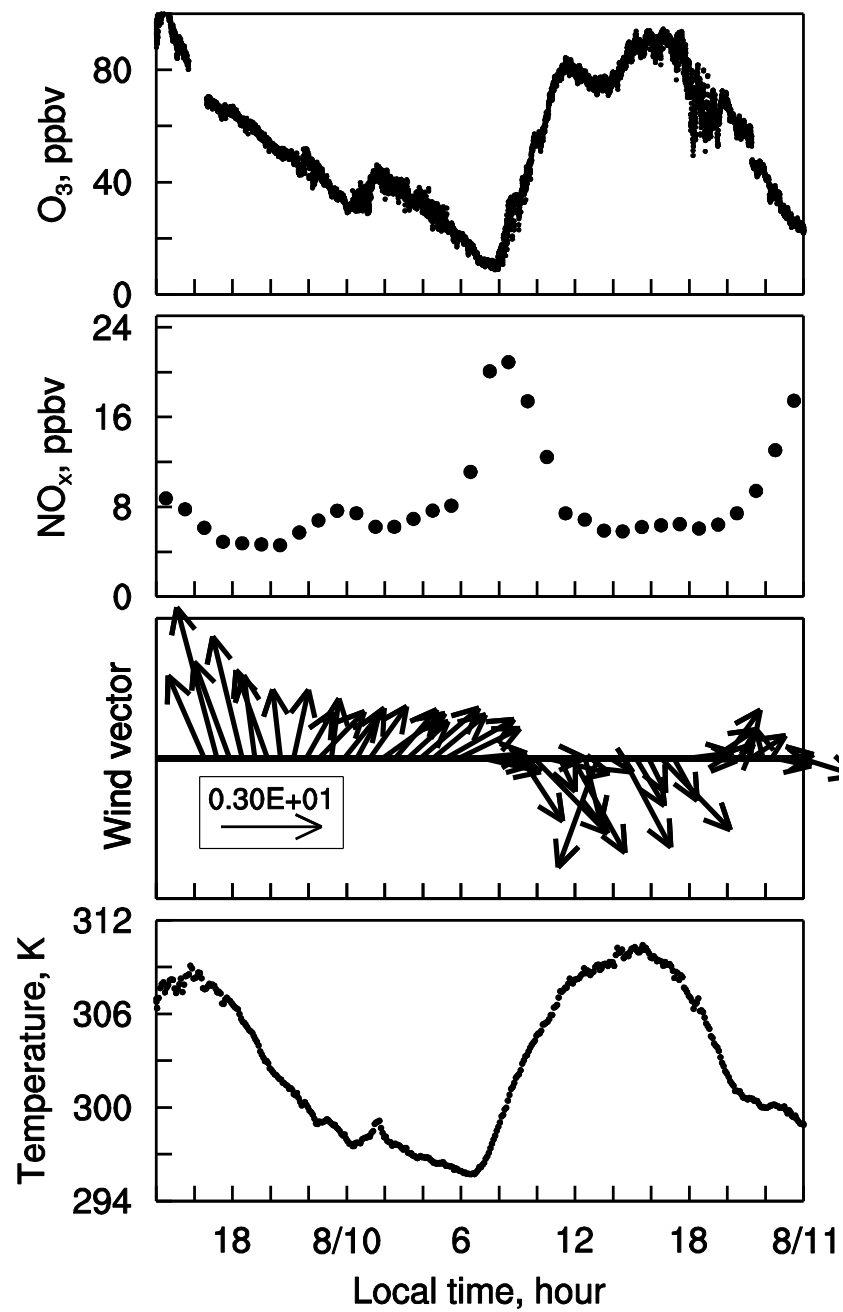


Figure 1. Observed (top to bottom) O₃, NO_x, wind vector, and temperature at Beltsville, Maryland on August 9-10, 2010.

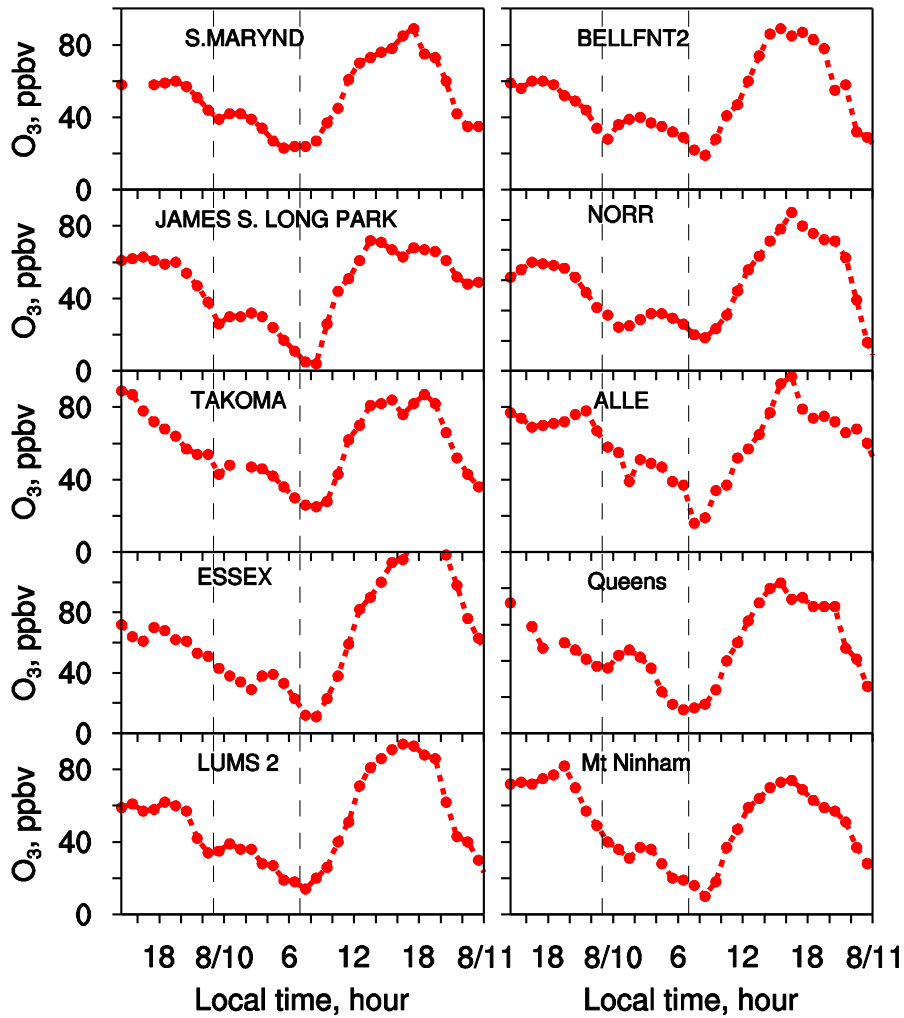


Figure 2. Time series of observed O_3 mixing ratios on Aug. 9-10, 2010 at 10 AIRNOW sites. The locations of these sites are marked in Fig. 3. The nighttime secondary O_3 maxima are confined in the time window between 2300 local time (LT), Aug. 9 and 0700 LT, Aug. 10, which are marked by the dashed lines.

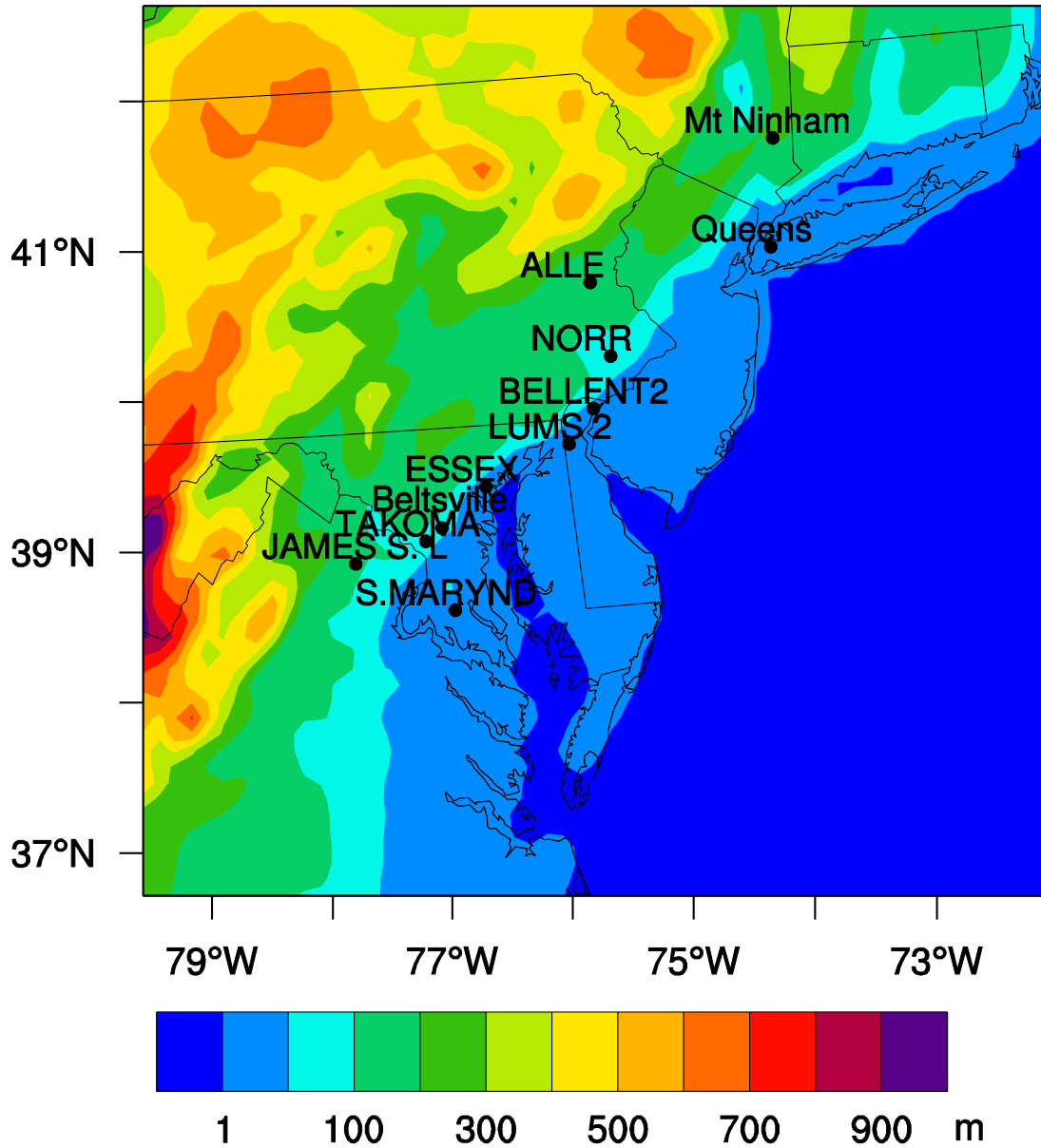


Figure 3. Terrain height of the study area. Locations of the AIRNOW sites are marked.

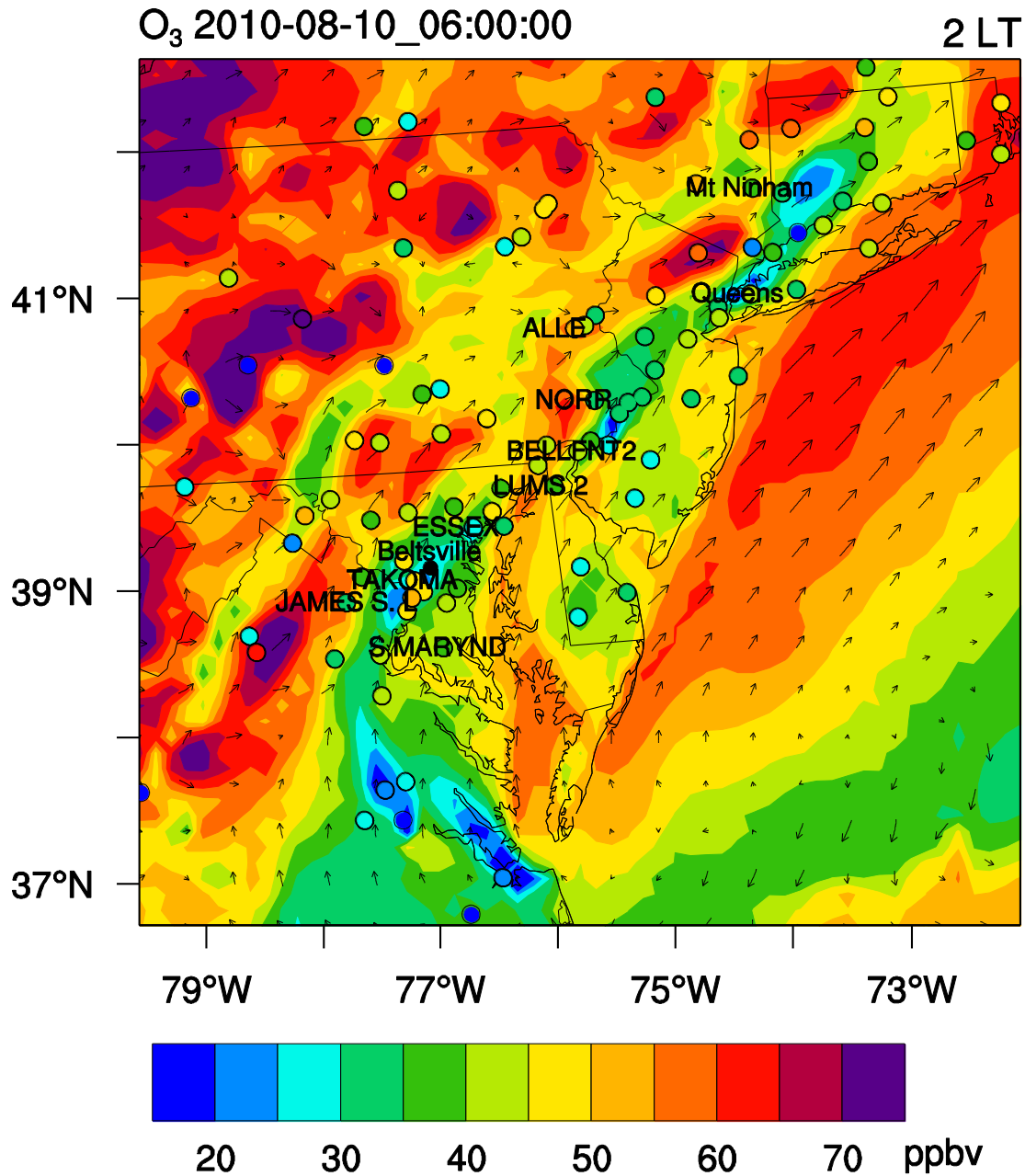


Figure 4. Spatial distribution of O₃ at 0200 local time (LT) on August 10, 2010 simulated by the WRF/Chem model. The observed O₃ values at the AIRNOW sites are indicated by shaded circles.

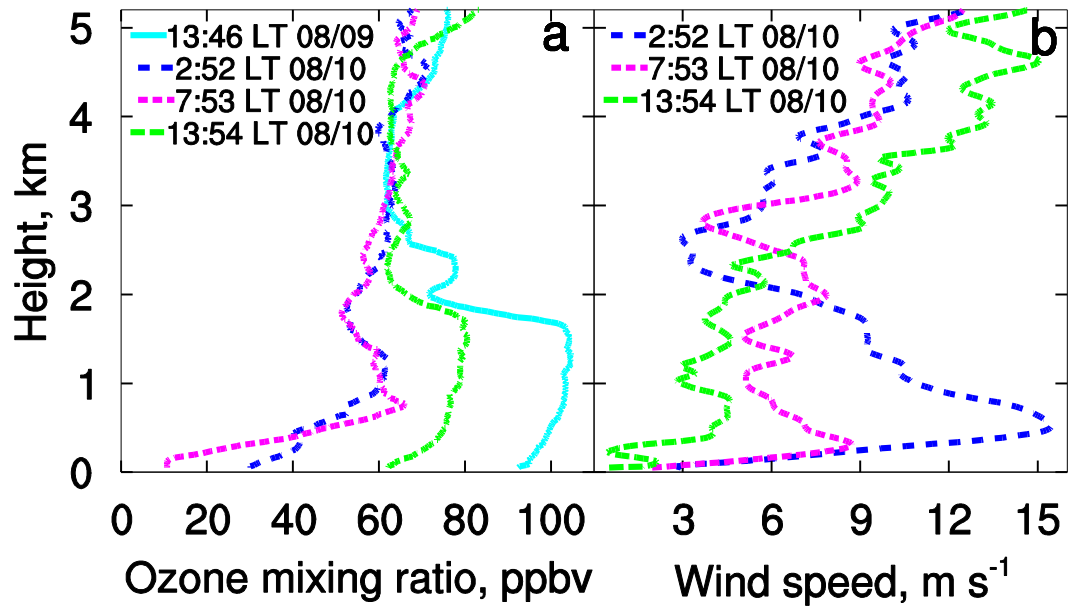


Figure 5. Observed vertical profiles of (a) O₃ and (b) wind speed at Beltsville, Maryland on August 9-10, 2010.

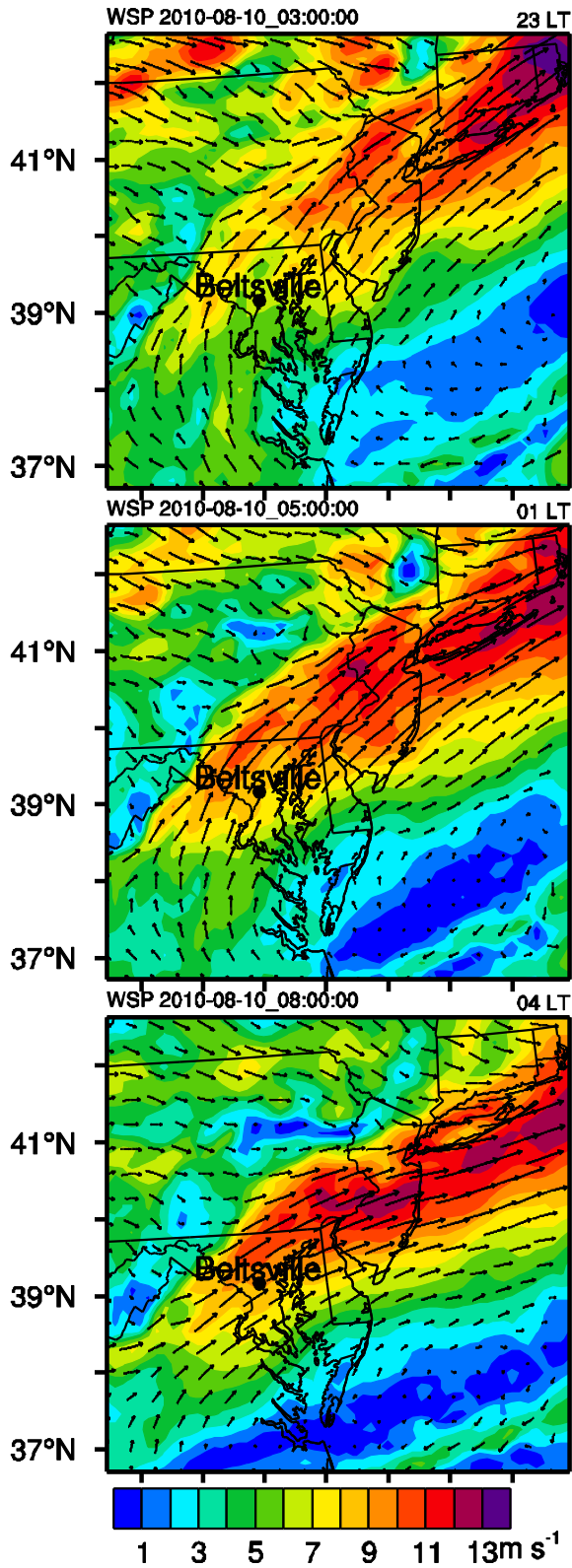


Figure 6. (top to bottom) Wind field at ~ 370 m AGL at 2300 LT on August 9, 0100 LT, and 0400 LT on August 10, 2010 simulated by WRF/Chem.

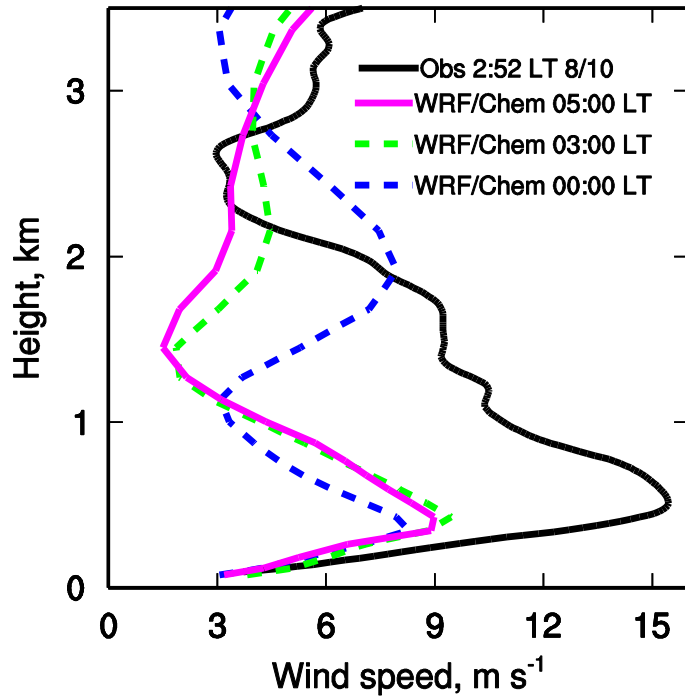


Figure 7. Simulated and observed vertical profiles of wind speed at Beltsville, Maryland on the night of August 9-10, 2010.

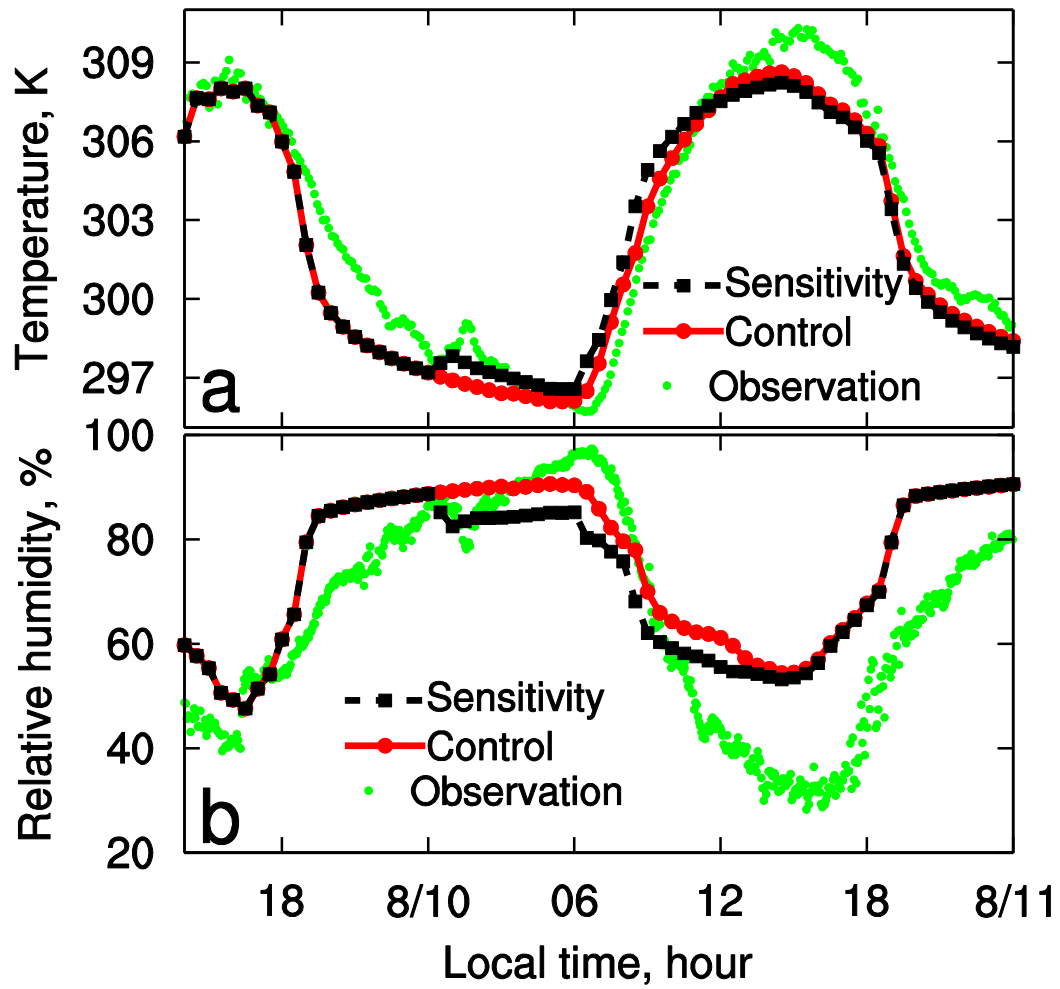


Figure 8. Observed and simulated time series of (a) temperature and (b) relative humidity near the surface.

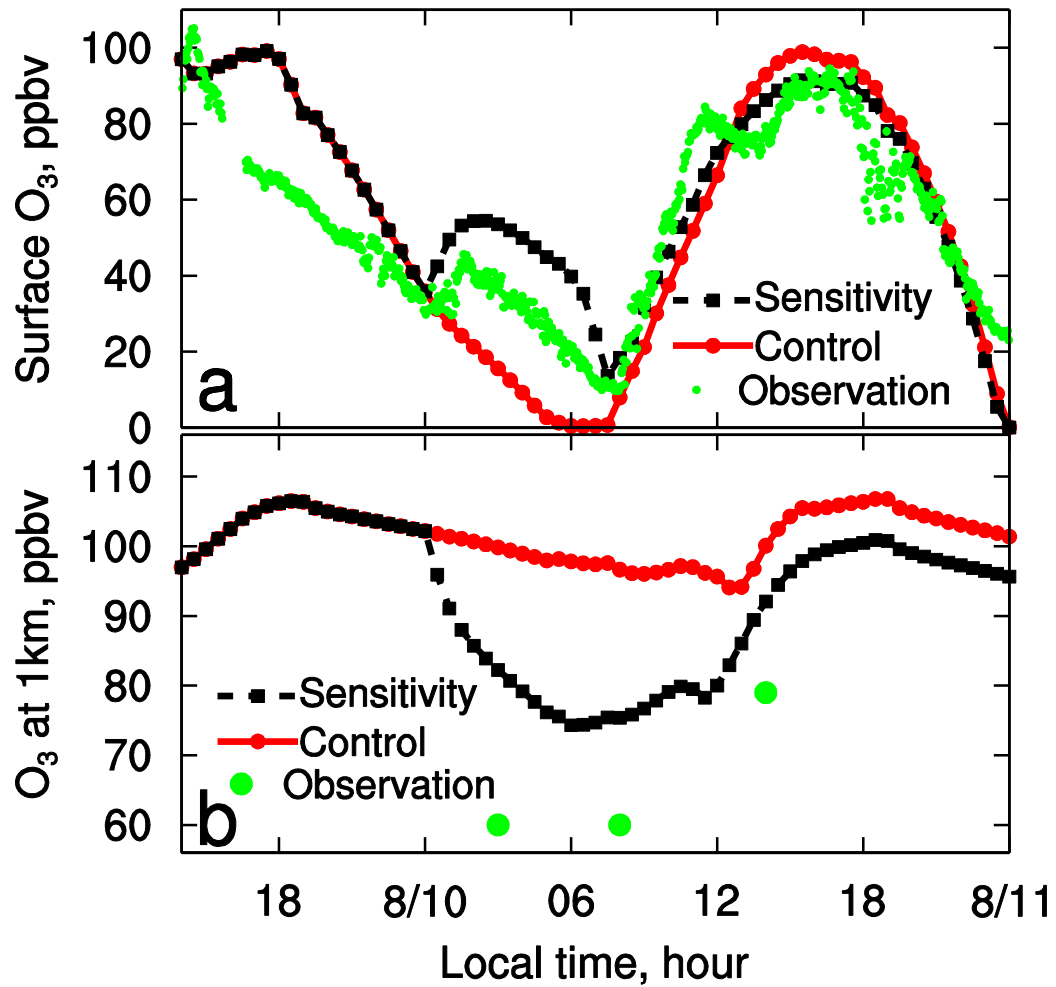


Figure 9. Time series of O₃ (a) near the surface and (b) at 1 km AGL (in the RL at night). Dots show observed O₃ near the surface (panel a) and observed O₃ at 1km AGL by Ozonesondes (panel b).

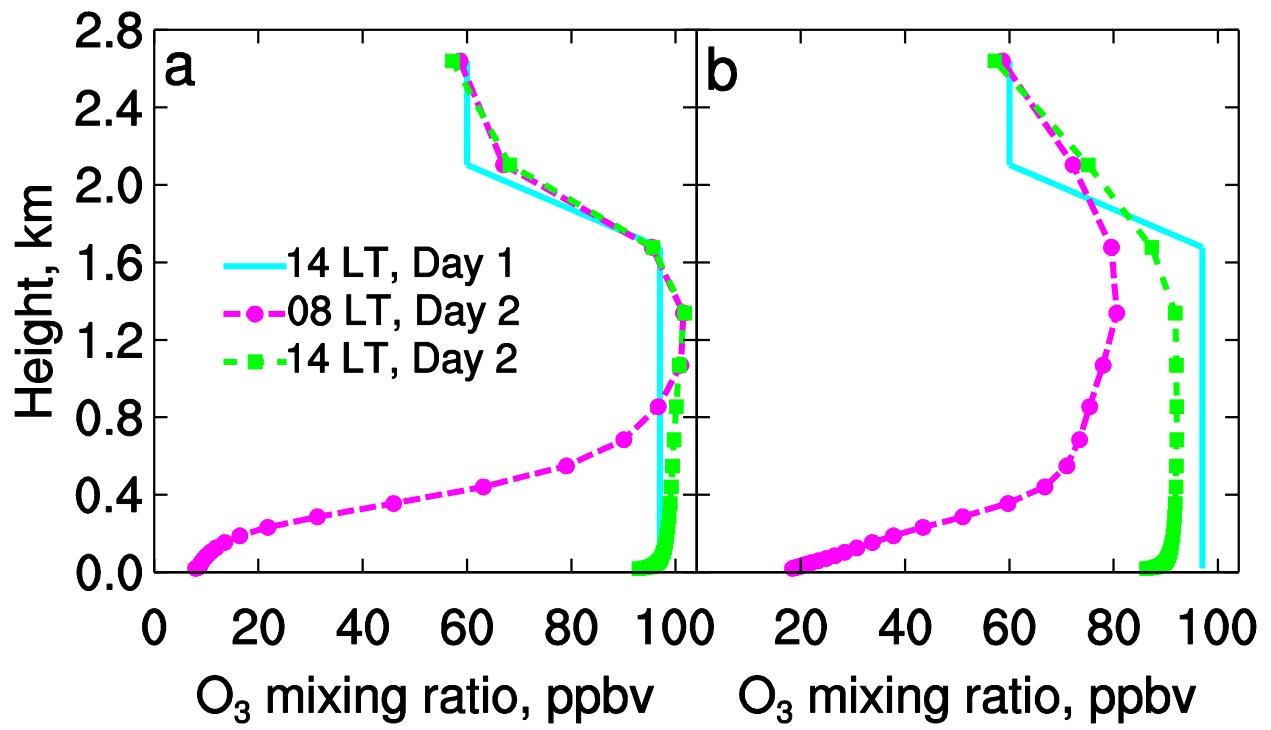


Figure 10. Profiles of simulated O₃ mixing ratio from (a) the control simulation and (b) sensitivity simulation.

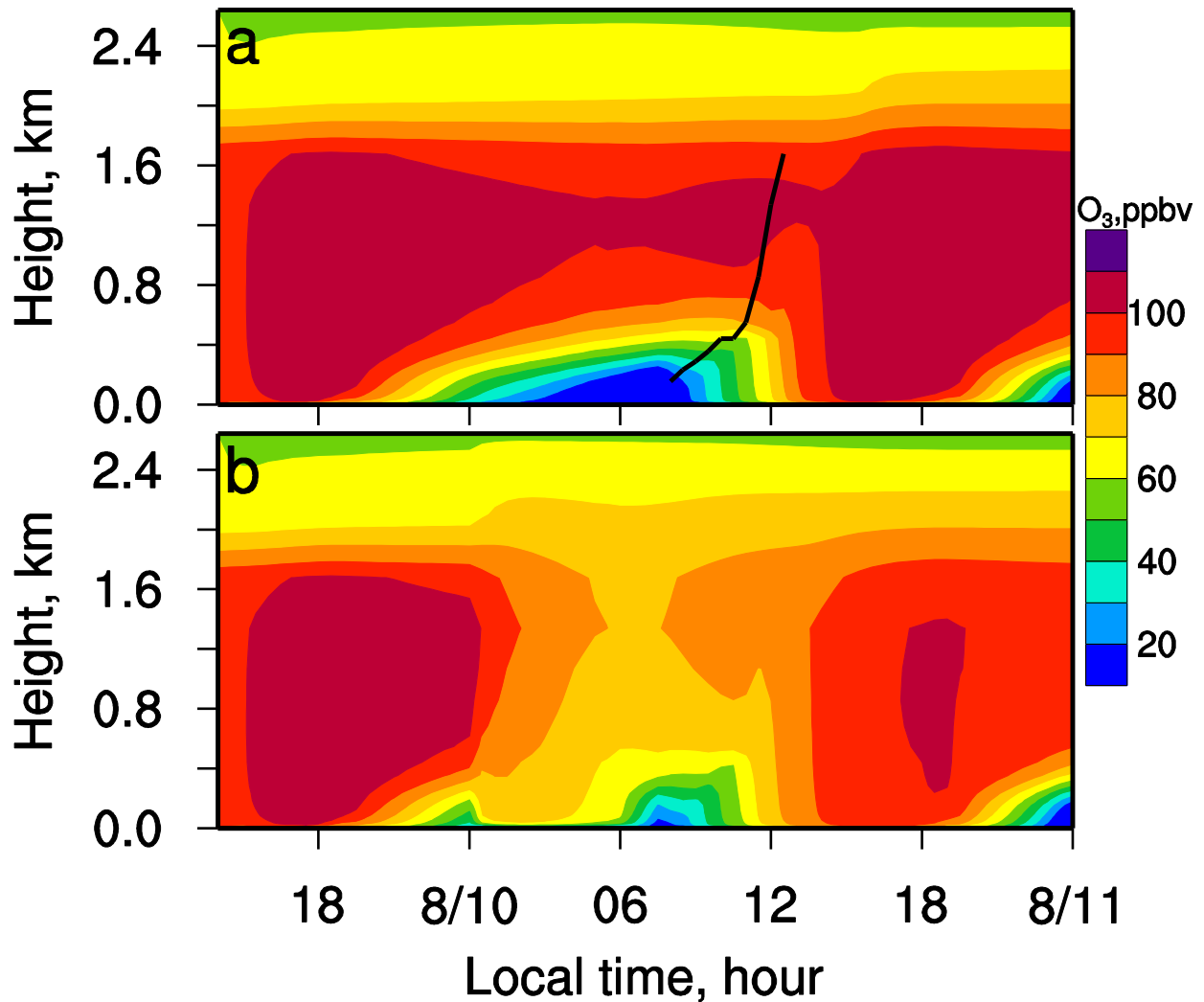


Figure 11. Time-height diagram of simulated O₃ mixing ratio from (a) the control simulation and (b) sensitivity simulation. The black line in the top panel indicates the top of the mixed boundary layer between 0730 and 1300 local time, which is diagnosed using the 1.5-theta-increase method (Hu et al., 2010). The 1.5-theta-increase method defines boundary layer top as the level at which the potential temperature first exceeds the minimum potential temperature within the boundary layer by 1.5 K.

1
2
3
4
5
6
7
8
9
10
11
12
13
14
15
16
17
18
19
20
21
22

**Impact of the Vertical Mixing Induced by Low-level Jets on Boundary Layer Ozone
Concentration**

Xiao-Ming Hu¹, Petra M. Klein^{1,2}, Ming Xue^{1,2},
Fuqing Zhang³, David C. Doughty³, Renate Forkel⁴, Everette Joseph⁵, and Jose D. Fuentes³

¹Center for Analysis and Prediction of Storms and ²School of Meteorology,
University of Oklahoma, Norman, Oklahoma, USA

³Department of Meteorology, Pennsylvania State University, University Park, Pennsylvania,
USA

⁴Karlsruher Institut für Technologie (KIT), Institut für Meteorologie und Klimaforschung,
Atmosphärische Umweltforschung (IMK-IFU), Kreuzeckbahnstr. 19, 82467 Garmisch-
Partenkirchen, Germany

⁵Department of Physics and Astronomy, Howard University, Washington, DC, USA

1st submitted on June 5, 2012

Revision on 9/12/2012 3:59 PM

23 **Abstract**

24 After sunset, a stable boundary layer (SBL) develops close to the ground, while the upper
25 region of the daytime mixed layer becomes the residual layer (RL). Mixing between the SBL
26 and RL is often quite limited and the RL is thought to be a reservoir for daytime mixed-layer
27 pollutants under such conditions. However, ozone (O_3) profiles observed in Maryland, U.S.
28 suggest that the RL is not always a reservoir of O_3 in that region. Nocturnal low-level jets
29 (LLJs) and/or other mechanisms are speculated to enhance vertical mixing between the SBL and
30 RL, which influences the vertical O_3 redistribution.

31 Nocturnal surface O_3 maxima, a RL with reduced O_3 levels, and a concurrent strong LLJ
32 were observed in Maryland on the night of August 9-10, 2010. Surface O_3 measurements in the
33 region and three-dimensional air quality simulations suggest that horizontal advection cannot
34 explain the nocturnal O_3 maxima and concurrent decrease of O_3 levels within the RL. A
35 sensitivity study with a single column (1D) chemistry model was performed to investigate the
36 role of LLJs in generating turbulent mixing within the nighttime boundary layer and to identify
37 related impacts on O_3 concentrations at night and on the following day. The strong shear
38 associated with the LLJ enhanced turbulent mixing and weakened the decoupling of the RL and
39 SBL substantially. Ozone was actively mixed down from the RL to the surface, causing
40 secondary nocturnal surface O_3 maxima. Near the surface, O_3 was efficiently removed by
41 chemical reactions and dry deposition, which resulted in lower O_3 peak values on the next day.

43 **1. Introduction**

44 Following the traditional picture of the diurnal evolution of the atmospheric boundary layer,
45 radiational cooling after sunset results in the development of a stable boundary layer (SBL) near
46 the surface that is typically quite shallow. Above the SBL is a residual layer (RL) with
47 characteristics similar to those of the previous day's mixed layer (Stull, 1988). In the absence of
48 strong disturbances, mixing and dispersion of pollutants between the RL and SBL become
49 limited, and within the RL the concentration of pollutants remains at similar levels as in the
50 mixed layer before its decay, which is why the RL is often viewed as a reservoir of pollutants
51 (Stull, 1988). The pollutants trapped within the RL from the previous day can be entrained
52 downward into the re-developing mixed layer on the following day. In places such as the
53 northeastern United States, such downward mixing of ozone (O_3) and its precursors is shown to
54 contribute substantially to ground-level O_3 buildup in the morning in addition to chemical
55 production (Zhang et al., 1998; Zhang and Rao 1999). The downward transport of the RL O_3 in
56 the morning also contributes to the maximum O_3 levels observed near the surface during daytime
57 (Neu et al., 1994; Aneja et al., 2000; Yorks et al., 2009; Morris et al., 2010; Tong et al., 2011).
58 Accurate information regarding the RL O_3 is thus critical for correctly simulating the daytime O_3
59 near the surface (Herwehe et al., 2011). Due to its relative inaccessibility, the actual detection of
60 the properties of the RL at high temporal and spatial scales has been limited in the past. Recent
61 field experiments (e.g., Balsley et al., 2008) showed that the classical view of a quiescent RL
62 may have been oversimplified. Sporadic turbulence exists at night, weakening the decoupling
63 between the RL and SBL, and the vertical mixing in the nighttime boundary layer may be
64 significant, even compared to that in the daytime convective boundary layer (Poulos et al., 2002;
65 Tjernstrom et al., 2009). Enhanced nighttime turbulence may be triggered by mesoscale motions

66 such as low-level jets (LLJ), Kelvin-Helmholtz instabilities, gravity waves, wake vortices, and
67 density currents (Sun et al., 2002, 2003; Salmond and McKendry, 2005; Fritts et al., 2009). Such
68 intense turbulence can affect the vertical structure of the nighttime boundary layer and vertical
69 distribution of pollutants. The view of the quiescent RL as a reservoir of pollutants may be
70 challenged under such conditions. Recent observations (Hu et al., 2012) have suggested that the
71 RL is leaky at times, i.e., active vertical exchange of air exists between the RL and the SBL. As
72 a result, the O₃ levels in the RL may be highly variable and surface O₃ may not decrease as fast
73 as anticipated based on the assumption of having a completely decoupled RL and SBL. In some
74 cases, there are even secondary nighttime O₃ maxima reported, which were typically associated
75 with periods of enhanced mixing (Corsmeier et al., 1997; Reitebuch et al., 2000; Salmond and
76 McKendry, 2002; Talbot et al., 2005; Hu et al., 2012). Therefore, it is important to further
77 investigate the dynamics and mixing of nocturnal boundary layers to better understand the
78 temporal variability, absolute levels, and deposition rates of surface layer O₃ concentrations.

79 In Beltsville, Maryland (MD), nighttime vertical O₃ profiles have been measured during the
80 summertime since 2004 (Yorks et al., 2009; Hu et al., 2012). Beltsville is located between
81 Washington, D.C. and Baltimore, MD, in the middle of the Mid-Atlantic urban corridor of the
82 United States. Heavy emissions of O₃ precursors and favorable meteorological conditions
83 frequently lead to extreme O₃ events in this area (Ryan et al., 1998). Within the RL, O₃ levels at
84 the Beltsville site at times resemble those found in the free troposphere with concentrations that
85 are significantly lower than those in the previous day's atmospheric mixed layer. Ozone in the
86 RL inherited from the daytime mixed layer appears to be readily mixed down to the surface,
87 contributing to elevated O₃ at night (Hu et al., 2012). Previous studies have shown that LLJs
88 occur frequently in the Mid-Atlantic region of the United States during the period between 1900-

89 0600 hours local time (LT), with peak winds ranging from 8 to 23 m s⁻¹ (Ryan, 2004; Zhang et
90 al., 2006). Such strong LLJs may cause the RL to become leaky (Banta et al., 2007). Thus, the
91 LLJs are hypothesized to contribute to the formation of leaky RL and nighttime surface O₃
92 maxima in the Mid-Atlantic region.

93 In the current study, the impacts of a LLJ observed in the Beltsville area on surface O₃ and
94 vertical O₃ profiles are investigated in detail using different numerical modeling approaches.
95 Initially, a three-dimensional model is employed to examine the spatial extent of the LLJ and to
96 diagnose its role in modulating boundary layer O₃. A single column model is then applied to
97 isolate the impacts of the LLJ on boundary layer mixing, nocturnal O₃ dispersion, and O₃ built-
98 up on the subsequent day. This study, for the first time, provides direct modeling evidence that
99 LLJs induce substantial turbulence and reduce the RL O₃ significantly; as a result, the O₃ level in
100 the daytime boundary layer on the following day is lowered.

101

102 **2. Methods**

103 During summer 2010, a research field campaign (Hu et al., 2012) was conducted at Howard
104 University's Atmospheric Research Site in Beltsville, MD (39.06°N, 76.88°W). The
105 meteorological variables and mixing ratios of chemical species (O₃, NO, NO₂, CO, SO₂) were
106 measured at 5 m above ground level (AGL). The mixing ratios of chemical species were
107 recorded every second. During several intensive observation periods, balloon-borne
108 meteorological and O₃ sondes were used to obtain vertical profiles of temperature, humidity,
109 wind speed and direction, and O₃. On the night of August 9-10, 2010, a secondary O₃ maximum
110 and a concurrent LLJ were observed at this research site. This event will be the focus of the
111 current study. In addition to the night of August 9-10, O₃ sondes were also launched in the

112 afternoon of August 9, which provided the unique opportunity during the field campaign to
 113 investigate the O₃ variation from the daytime convective boundary layer to the nighttime
 114 boundary layer. LLJs commonly occur in the Mid-Atlantic region (Zhang et al., 2006). This case
 115 study demonstrates potential impacts of the frequently occurring phenomenon of nocturnal LLJs
 116 on boundary layer O₃.

117 Three-dimensional (3D) air quality simulations, using the Weather Research and Forecasting
 118 model with Chemistry (WRF/Chem, Grell et al., 2005), for the 2010 summer campaign were
 119 applied in Hu et al. (2012) to investigate regional transport of O₃ and illustrate certain caveats in
 120 3D air quality simulations. As part of the current study, output from these WRF/Chem
 121 simulations along with hourly O₃ data recorded at the AIRNOW sites in the region were first
 122 used to examine the spatial extent and the potential causes of elevated nocturnal surface O₃
 123 concentrations during the night of August 9-10, 2010. Details about the model set-up and
 124 domains of the WRF/Chem simulations can be found in Hu et al. (2012).

125 To further investigate the impacts of the strong LLJ observed on the night of August 9-10,
 126 2010 near the Beltsville site on the vertical distribution of O₃, a single column photochemical
 127 model CACHE (Forkel et al., 2006) is employed in this study. In the vertical direction, 40 model
 128 layers extend from the surface to the 2.64-km height, with a vertical grid spacing of 1 m for the
 129 lowest layer and 500 m for the uppermost layer; such a setup appears to adequately capture the
 130 boundary layer structure during both nighttime and daytime. The multi-layered photochemical
 131 model solves the following system of equations:

$$132 \quad \frac{dC_{ij}}{dt} = -C_{ij} \sum_k P_{kj} + \sum_k P_{kj} C_{kj} - C_{ij} \sum_k R_{kj} + \sum_k R_{kj} C_{kj} \quad (1)$$

133 where subscripts *i* and *j* denote the *i*th chemical species and the *j*th model layer, respectively, with

134 χ being the concentration of a chemical species. Terms E , D and C are the rates of change due
135 to emissions, dry deposition, and chemical reactions, respectively. The estimation method of
136 emissions of volatile organic compounds, E , was updated to use the formula of Guenther (2006).
137 The dry deposition, D , is treated using the methods of Wesely (1989) and Gao et al. (1993). The
138 chemical reaction rate, C , is computed using the Regional Atmospheric Chemistry Mechanism
139 (RACM) gas-phase mechanism (Stockwell et al., 1997). The atmospheric turbulent transport
140 term, i.e., the last term of (1), is parameterized using a first-order closure scheme. The eddy
141 diffusivity K is described using a mixing-length approach, in which K is expressed as a function
142 of mixing length l , the vertical wind shear $\partial u / \partial z$, and the stability function f :

$$(2)$$

144 This first-order parameterization is widely applied in operational NWP and climate models
145 (Beare et al., 2006; Cuxart et al., 2006). The stability function f is parameterized using the
146 Richardson number Ri ; a larger/smaller Ri leads to a smaller/larger value of the stability function.
147 The Richardson number Ri , a dynamic stability parameter, represents the ratio of thermally to
148 mechanically produced turbulence in a defined air layer.

149 Two simulations are conducted with the single column model. In the control simulation,
150 a calm condition (no LLJ) is considered while in a sensitivity simulation a LLJ is included. The
151 simulations are initialized at 1400 LT on August 9, 2010, and run for 34 hours. The initial
152 concentrations of O_3 and nitrogen oxides (NO_x) come from field observations while the initial
153 concentrations of other species come from the WRF/Chem simulation conducted in Hu et al.
154 (2012). The shortwave radiation is constrained by the observed values. The simulated mixing
155 ratio of NO_x in the boundary layer is nudged to the observed values at 5m AGL every half-hour.
156 Advection is not considered in the single column model. The boundary layer advection pathway

157 in Maryland changed during the daytime of August 10, 2010 (Hu et al., 2012). Thus bias of the
158 simulated mixed layer O₃ on August 10 by the single column model is expected. However, the
159 goal of the single column model simulations is to isolate the impact of the vertical mixing
160 induced by a LLJ on boundary layer O₃ by examining the difference between the control and the
161 sensitivity simulations.

162 163 **3. Observations and three-dimensional WRF/Chem simulations**

164 The measured O₃, NO_x and the corresponding meteorological variables on August 9-10,
165 2010 at the Beltsville research site, 5 m AGL, are shown in Fig. 1. Due to the diurnal cycle of
166 photochemical production, O₃ maxima typically occur in the afternoon in the continental
167 atmospheric boundary layer. During summer nights, NO_x mixing ratios are ~7 ppbv and NO
168 titration and dry deposition usually result in continuously decreasing O₃ concentrations near the
169 surface in Beltsville (Hu et al., 2012). During our study period, however, a secondary O₃
170 maximum was recorded on the night of August 9-10, 2010; O₃ mixing ratios between 0000 and
171 0300 LT were elevated by ~15 ppbv. By 0700 and 0800 LT, the O₃ mixing ratio decreased to
172 ~10 ppbv due to NO titration and dry deposition. The secondary O₃ maximum was accompanied
173 by a decrease of the NO_x mixing ratio and increase of temperature. Southwesterly winds (~2 m
174 s⁻¹) were maintained during the period of 0000-0500 LT, suggesting that a similar footprint and
175 air mass persisted during this period. These factors suggest that the secondary O₃ maximum at
176 the surface on the night of August 9-10, 2010 was due to downward mixing of RL O₃, as was
177 also reported in Talbot et al. (2005) and Hu et al. (2012). Since the upper layers typically had
178 higher O₃ mixing ratios, lower NO_x mixing ratios, and higher potential temperatures, one can
179 conclude that vertical mixing between the SBL and RL persisted during the night, which led to

180 an increase in surface O₃ and temperature, and a decrease in surface NO_x.

181 Similar secondary nocturnal O₃ maxima were also recorded at the majority of AIRNOW
182 sites (60% of 45 sites) along the Virginia-to-Connecticut corridor on the same night. Other
183 AIRNOW sites along this corridor also experienced elevated O₃ on this night, but an isolated
184 secondary O₃ maximum was not apparent. The concentration variations for ten exemplary sites
185 are shown in Fig. 2. Figure 3 illustrates the locations of those sites. These AIRNOW sites are
186 located across a wide region with different characteristics such as urban and rural land use types.
187 Their upstream O₃ mixing ratios varied significantly according to the WRF/Chem simulation
188 (Fig. 4), which can be explained by the different elevation of the monitoring sites (Fig. 3) and
189 spatially variable precursor emission rates within the domain. Ozone was removed more
190 efficiently by NO titration around anthropogenic emission sources such as big cities and traffic
191 roads. Factors contributing to higher nighttime O₃ concentrations at elevated locations (e.g., in
192 the Appalachian Mountains) included (1) a more explicit influence of O₃-richer air from the free
193 troposphere, (2) lower anthropogenic emission rates, and (3) limited transport of NO into these
194 regions. Despite the heterogeneous upstream O₃ mixing ratios, almost concurrent nocturnal
195 secondary O₃ maxima were observed at the AIRNOW sites along the Virginia-to-Connecticut
196 corridor. Given the large variability in O₃ concentrations near each site, advection cannot
197 explain these nearly simultaneous secondary maxima. The distance between the south-west (S.
198 MARYND) and north-east (Mt Ninham) sites along the corridor is ~600 km. Even with a wind
199 speed as high as 20 m s⁻¹, it would take more than eight hours for an air mass to travel across this
200 distance. The secondary O₃ maximum at Mt Ninham would be expected to occur several hours
201 later than at the S. MARYND site if they were due to advection of an O₃-richer air mass, which
202 was clearly not observed. Given the difficulties in reproducing the structure of the nocturnal

203 boundary layer and nighttime chemistry, the simulated vertical profile of chemical species can be
204 biased (Zhang et al., 2009; Herwehe et al., 2011; Hu et al., 2012). Thus, the results from the
205 WRF/Chem simulations should not be over interpreted. It can be noted, however, that the
206 general O₃ patterns remain similar throughout the entire period from 0000 LT to 0400 LT
207 (Figure not shown), which is another indication that advection did not play a crucial role in the
208 formation of the nighttime secondary O₃ maxima. The small variations in the onset times of the
209 secondary O₃ maxima among the ten sites (Fig. 2) do not show any systematic trends related to
210 the position of the site along the SW-NE corridor. They can likely be explained by the local
211 characteristics of each site (e.g., urban vs. rural and different elevation), which resulted in
212 different nocturnal O₃-depletion rates, vertical O₃ distributions, and turbulent mixing at each site.

213 Boundary layer structures on August 9-10, 2010 are clearly illustrated by the measured
214 vertical profiles of O₃ (Fig. 5a). During daytime, elevated O₃ mixing ratios due to photochemical
215 production are confined in the mixed layer, which is the lower ~1.7 km AGL. The O₃ mixing
216 ratio in the daytime mixed layer on August 9, 2010 was as high as 100 ppbv (Fig. 5a). During
217 nighttime, strong vertical gradients of O₃ mixing ratios develop in the stable boundary layer (~
218 600 m AGL) due to efficient O₃ removal by NO titration and dry deposition near the surface. If
219 the stable boundary layer developing near the surface is decoupled from the RL, we would
220 expect to observe low O₃ concentrations close to the surface, but concentrations inside the RL
221 would remain close to the values observed within the previous day mixed layer (~100 ppbv in
222 the studied case). However, O₃ concentrations decreased throughout the RL (0.8-1.7 km AGL)
223 on the night of August 9-10, 2010 to as low as 50-60 ppbv, which more closely resemble the
224 values in the free troposphere. The decrease of the RL O₃ concentrations by nearly a factor of 2
225 compared to the previous day mixed-layer values, confirms that active dispersion of RL O₃

226 persisted on this night. At the same time, a strong LLJ over the Beltsville research site was
227 recorded during the study period. The wind speed exceeded 15 m s^{-1} at 500 m AGL at 0252 LT
228 on August 10 (Fig. 5b). Along the western, mountainous side of the Virginia-to-Connecticut
229 corridor, strong radiative cooling near the ground results in lower nighttime temperatures than on
230 the eastern side. Such a horizontal temperature gradient, caused by the terrain effects (Fig. 3),
231 can induce a southwesterly thermal wind in the nocturnal boundary layer (Ryan, 2004), and
232 contribute to the formation of the nighttime LLJ. The meridional variation of the Coriolis
233 parameter could also accelerate the northward-blowing LLJ (Wexler, 1961; Zhong et al., 1996).
234 The results from WRF/Chem simulations reported in Hu et al. (2012) also showed that a
235 persistent low-level jet formed east of the Appalachian Mountains over the Virginia-to-
236 Connecticut corridor (Fig. 6). Compared with the observed wind profiles, the maximum LLJ
237 wind speed was however significantly underestimated by WRF (Fig. 7). Beltsville and all the
238 sites experiencing secondary O_3 maximum shown in Fig. 2 are located in the corridor affected by
239 the LLJ. As it was already discussed, neither the observations nor the model results indicate that
240 advection of O_3 triggered the secondary, nighttime O_3 maxima. Instead, it is hypothesized that
241 the LLJ induced strong turbulence, which weakened the decoupling between the SBL and RL
242 and triggered enhanced mixing of O_3 from the RL to the ground, causing the observed increase in
243 surface O_3 . To prove this hypothesis, a one-dimensional modeling study was conducted that
244 allowed us to isolate the role of the LLJ.

245

246 **4. Impact of LLJ-induced vertical mixing in one-dimensional simulations**

247 The 3D WRF/Chem simulation predicted that a LLJ formed and persisted throughout the
248 early morning hours. However, it significantly underestimated the strength of the LLJ (Fig. 7),

249 which meant that the WRF/Chem model would not accurately reproduce the vertical mixing in
250 the NBL. However, even if the simulation had correctly reproduced the LLJ strength, it would
251 still be difficult to identify the contribution of the LLJ in moderating the vertical O₃ distribution
252 because the interplay of several processes (e.g., vertical mixing and horizontal advection) cannot
253 be easily separated in 3D simulations. Therefore, simulations are conducted in this study using a
254 single-column model to examine the impact of LLJ-induced vertical mixing on August 10, 2010.
255 The environmental wind profile is manually set up in the model using the observed wind profile
256 as guidance. Two simulations are conducted; the control simulation has a calm condition while a
257 sensitivity experiment has a LLJ profile between 0000 LT and 0600 LT of day 2; the latter is
258 otherwise the same as the control simulation. The maximum wind speed (WSP) of the LLJ at
259 440 m AGL is set as 20 m s⁻¹. The single column model does not consider directional wind
260 shear. Instead, the maximum WSP of the LLJ is set at a higher value than the observation to
261 account for the effect of directional shear-induced turbulence.

262 The simulations with the single column model captured the meteorological conditions (e.g.,
263 temperature and relative humidity) reasonably well (Fig. 8). In the sensitivity simulation, the
264 impacts of LLJ-induced vertical mixing on meteorological conditions near the surface are
265 successfully captured. An abrupt increase of temperature and decrease of relative humidity near
266 the surface are reproduced at the onset of the LLJ, i.e., 0000 LT on August 10, 2010.

267 The simulated time series of O₃ mixing ratios near the surface are shown in Fig. 9a. At the
268 onset of the LLJ (0000 LT), O₃ mixing ratios near the surface increased by ~18 ppbv in the
269 sensitivity simulation. At the same time, surface temperature increased (Fig. 8). These results
270 are consistent with the observed secondary O₃ maximum shown in Fig. 1. The surface O₃ was
271 nearly depleted on the calm night in the control simulation due to dry deposition and NO titration,

272 while it was elevated in the sensitivity simulation with the LLJ (Fig. 9a). Such difference of the
273 surface O₃ caused by LLJs was also reported in previous studies (Banta et al., 2007). These
274 results therefore confirm the hypothesis that the LLJ played an important role in downward
275 mixing of O₃ during the night of August 9-10, 2010.

276 The simulated vertical profiles of O₃ are shown in Fig. 10. The LLJ played an important role
277 in removing O₃ in the RL at night. According to the formula (2), elevated wind shear in the
278 presence of the LLJ will cause an increase of the eddy diffusivity. As a result of the shear-
279 enhanced turbulence, the temperature inversion weakened, *Ri* further decreased, which,
280 according to (2), as a whole contributed to a substantial increase in eddy diffusivity in the
281 presence of a LLJ. The enhanced vertical mixing played a critical role in modulating the vertical
282 redistribution of O₃ in the boundary layer. On a calm night, O₃ in the RL was mostly conserved
283 while the RL O₃ was reduced by ~25 ppbv at 0800 LT in the presence of the LLJ (Fig. 10 and
284 Fig. 9b). LLJs have also been reported to induce mechanical turbulence that can vertically mix
285 O₃ in the nocturnal boundary layer in other regions such as Texas (Tucker et al., 2010). The
286 significant reduction of O₃ in the RL in both observations (Fig. 5a) and simulation (Fig. 10b)
287 indicates that the RL may not be a reservoir of pollutants in the presence of strong LLJs. The
288 simulated reduction of the RL O₃ from the daytime mixed layer by the sensitivity simulation
289 (~25 ppbv, Fig. 10b) was smaller than the observed reduction (~40 ppbv, Fig. 5a). Such
290 discrepancy may be due to the exclusion of advection processes in the single column model
291 and/or model errors. Model errors in the treatments of vertical mixing in meteorological and air
292 quality models are shown to lead to substantial bias of simulated profiles of meteorological and
293 chemical variables (Hu et al., 2010, 2012; Nielsen-Gammon et al., 2010).

294 Due to the enhanced turbulence induced by the LLJ, more O₃ was transported to the surface,
295 where it was subjected to NO titration and enhanced dry deposition. The dry deposition velocity
296 was correlated to the friction velocity u_* , with larger u_* values leading to larger dry deposition
297 velocities. Enhanced turbulent mixing in the presence of a LLJ resulted in an increase in u_* , and
298 thus higher dry deposition rates. As a result, the LLJ affected the O₃ budget at night, which in
299 turn affected the O₃ concentration in the daytime mixed layer on the following day. Figure 10
300 shows that the mixed-layer O₃ at 1400 LT on the second day was reduced by ~8 ppbv due to the
301 influence of the LLJ compared to the control simulation without the LLJ. The simulated
302 maximum surface O₃ on August 10, 2010 was reduced by ~8 ppbv with the LLJ while the
303 maximum 8-hour running average O₃ was reduced by ~6 ppbv (Fig. 9a). Compared with the
304 observed O₃ profile at 13:54 LT on August 10 (~80 ppbv in the mixed layer), the predicted O₃ in
305 the mixed layer on the second day by the sensitivity simulation is higher by ~10 ppbv. The
306 discrepancy is likely due to the change of transport pathways during the daytime of August 10,
307 2010 (Hu et al., 2012), which is not considered in the single column model.

308 The time-height diagrams of simulated O₃ are shown in Fig. 11. Without the LLJ, the RL O₃
309 is mostly conserved (Fig. 11a). When the daytime mixed layer grows, the O₃-rich RL air is
310 entrained into the mixed layer below, thereby contributing to the rapid increase in O₃ in the
311 mixed layer in the morning. Such a scenario is described in Zhang and Rao (1999) and
312 confirmed by other studies (Aneja et al., 2000; Yorks et al., 2009; Morris et al., 2010; Tong et
313 al., 2011). However, in the presence of the LLJ, the RL O₃ is removed at night (Fig. 11b). In the
314 following morning, entrainment contributes much less to the O₃ in the mixed layer (Fig. 11b),
315 thus the increase of surface O₃ is much slower comparing to the control simulation (Fig. 9a).

316

317 **5. Conclusions and discussion**

318 Profiles of O₃ and meteorological variables in both nighttime and daytime have been
319 measured in summertime since 2006 in Beltsville, Maryland (Hu et al., 2012). The data sets
320 provided a unique opportunity to investigate the pollutants in the residual layer (RL) and their
321 contribution to the daytime boundary layer pollution. It is shown that the RL was at times not a
322 reservoir of O₃ at night. A case study was conducted for August 9-10, 2010, when a strong LLJ
323 and elevated surface O₃ were observed at night. During this night, the RL O₃ was 50-60 ppbv,
324 which was much lower than the O₃ level in the mixed layer on the previous day (~100 ppbv).
325 Thus, O₃ appeared to be mixed from the RL to the ground preventing the RL from acting like a
326 reservoir. Simulation results from a single-column model containing O₃ chemistry confirm that
327 the LLJ causes a nocturnal secondary O₃ maximum and a significant reduction of the RL O₃.
328 The LLJ-induced strong turbulence, which transports O₃-rich RL air to the surface where O₃ is
329 efficiently removed by chemical reactions and enhanced dry deposition. These processes impact
330 the O₃ budget: the enhanced nocturnal vertical mixing reduces the increase in surface O₃ the
331 following morning and, compared to the results of a control simulation with calm conditions, the
332 maximum O₃ is ~ 8 ppbv lower for the simulation containing a LLJ.

333 Salmond and McKendry (2002) found that secondary surface O₃ maximum due to enhanced
334 nocturnal mixing rarely exceeded 50 ppbv. They concluded that the nocturnal secondary O₃
335 maximum is unlikely to be significant enough to affect human health. Our study shows that such
336 nocturnal mixing may play an important role in modulating the O₃ levels in the daytime
337 boundary layer on the following day; it may thus have a more important implication for public
338 health than it had been previously realized.

339 Ryan (2004) investigated the climatology of LLJs in Maryland, USA and found that the
340 weather patterns favorable for the development of LLJs are normally also suitable for the
341 occurrence of Mid-Atlantic high O₃ episodes. Thus, the influence of LLJs on the O₃ episodes
342 can be hardly discerned from other factors that are conducive to O₃ accumulation. Due to the
343 difficulty in accurately reproducing LLJs and the interplay of several processes (e.g., vertical
344 mixing and horizontal advection) in three dimensional air quality simulations, a previous study
345 on this case (Hu et al. 2012) did not isolate the impact of LLJs on the vertical distribution of O₃.
346 Using a single column chemistry model that allows for easier setup of sensitivity experiments in
347 this study, the impact of LLJs on the boundary layer O₃ pertaining to stronger vertical mixing is
348 isolated. The effects of horizontal long-range transport due to LLJs are not considered in this
349 study. One implication of this study for long-range transport is: the pollutants in the RL may
350 leak out during the horizontal transport due to enhanced vertical mixing, reducing the impact of
351 urban plumes in downwind areas.

352 LLJs have been reported in many regions (Whiteman et al., 1997; Song et al., 2005; Zhang et
353 al., 2006); the LLJs in other regions (e.g., the Great Plains of the United States) may be much
354 stronger and more extensive than those in the Mid-Atlantic region (Zhang et al., 2006). Thus,
355 the impact of LLJs on the boundary layer O₃ may have important implications for air quality in
356 many regions. Apart from LLJs, mesoscale motions such as Kelvin-Helmholtz instabilities,
357 gravity waves, wake vortices, and density currents can also cause enhanced nighttime turbulence
358 (Sun et al., 2002, 2003; Salmond and McKendry, 2005; Fritts et al., 2009), which may also make
359 the RL leaky. In addition to O₃, nocturnal mixing events may have appreciable effects on the
360 dispersion and budget of other species such as carbon dioxide and volatile organic compounds
361 (Acevedo et al., 2006; Ganzeveld et al., 2008). In one-dimensional simulations for the boundary

362 layer over a tropical forest using a single column chemistry-climate model, Ganzeveld et al.
363 (2008) showed that unresolved nocturnal vertical mixing processes likely lead to a nocturnal
364 accumulation of formaldehyde in the RL, which is later on entrained into the daytime convective
365 boundary layer where it affects daytime photochemistry. Further investigations regarding such
366 mixing processes and their impacts are warranted. Future field campaigns that aim at improving
367 our understanding of atmospheric chemistry in the atmospheric boundary layer should include
368 measurements of the chemical composition/transformation in combination with detailed
369 measurements of turbulence inside the RL.

370 Although the current study focuses on demonstrating the importance of vertical mixing
371 processes for vertical dispersion of boundary layer O₃, the contribution of other processes,
372 including advection (Banta et al., 2005; Zhang et al. 2007; Tucker et al., 2010), dry deposition
373 (Lin and McElroy, 2010) and chemical reactions in different chemical regimes at different height
374 above the ground (Brown et al., 2007), cannot be always ignored. To more accurately quantify
375 their contributions, meteorological and air chemistry measurements throughout the atmospheric
376 boundary layer are needed to further improve boundary-layer parameterizations, particularly for
377 nighttime conditions, and to facilitate the development and evaluation of more sophisticated
378 three-dimensional chemistry simulations.

379
380 *Acknowledgement.* This work was supported by funding from the Office of the Vice President
381 for Research at the University of Oklahoma. The second author was also supported through the
382 NSF Career award ILREUM (NSF ATM 0547882). DCD received support from NASA (grant
383 number NNX08BA42A) to participate in the field studies. JDF received support from the
384 National Science Foundation to participate in this research (award ATM 0914597).

385 *Observations at Howard University Beltsville Campus were supported through grants from*
386 *Maryland Department of the Environment, NASA (grant number NNX08BA42A) and NOAA*
387 *(grant number NA17AE1625).*

388 **References**

389 Acevedo, O. C., Moraes, O. L. L., Degrazia, G. A., Medeiros, L. E., 2006. Intermittency and the
390 exchange of scalars in the nocturnal surface layer. *Boundary-Layer Meteorology* 119, 41–55.

391 Aneja, V. P., Mathur, R., Arya, S. P., Li, Y., Murray, G. C., Manuszak, T. L., 2000. Coupling the
392 vertical distribution of ozone in the atmospheric boundary layer. *Environmental Science &*
393 *Technology* 34, 2324–2329.

394 Balsley, B., Svensson, G., Tjernström, M., 2008. On the scale dependence of the gradient
395 Richardson number in the residual layer. *Boundary-Layer Meteorology* 127, 57–72.

396 Banta, R. M., Seniff, C. J., Nielsen-Gammon, J., Darby, L. S., Ryerson, T. B., Alvarez, R. J.,
397 Sandberg, S. P., Williams, E. J., Trainer, M., 2005. A Bad Air Day in Houston. *Bulletin of*
398 *American Meteorological Society* 86, 657-669.

399 Banta, R. M., Mahrt, L., Vickers, D., Sun, J., Balsley, B. B., Pichugina, Y. L., Williams, E. J.,
400 2007. The Very Stable Boundary Layer on Nights with Weak Low-Level Jets. *Journal of the*
401 *Atmospheric Sciences* 64, 3068–3090.

402 Beare, R. J., et al., 2006. An intercomparison of large-eddy simulations of the stable boundary
403 layer. *Boundary-Layer Meteorology* 118(2), 247–272.

404 Brown, S.S., Dube, W.P., Osthoff, H.D., Wolfe, D.E., Angevine, W.M., Ravishankara, A.R.,
405 2007. High resolution vertical distributions of NO₃ and N₂O₅ through the nocturnal boundary
406 layer. *Atmospheric Chemistry and Physics* 7, 139–149.

407 Corsmeier, U., Kalthoff, N., Kolle, O., Kotzian, M., Fiedler F., 1997. Ozone concentration jump
408 in the stable nocturnal boundary layer during a LLJ-event. *Atmospheric Environment* 31,
409 1977-1989.

410 Cuxart, J., et al., 2006. Single-column model intercomparison for a stably stratified atmospheric
411 boundary layer. *Boundary-Layer Meteorology* 118, 273–303.

412 Forkel, R., Klemm, O., Graus, M., Rappengluck, B., Stockwell, W. R., Grabmer, W., Held, A.,
413 Hansel, A., Steinbrecher, R., 2006. Trace gas exchange and gas phase chemistry in a Norway
414 spruce forest: A study with a coupled 1-dimensional canopy atmospheric chemistry emission
415 model. *Atmospheric Environment* 40, 28–42.

416 Fritts, D. C., Wang, L., Werne, J., 2009. Gravity wave–fine structure interactions: A reservoir of
417 small-scale and large-scale turbulence energy. *Geophysical Research Letters* 36, L19805,
418 doi:10.1029/2009GL039501.

419 Gao, W., Wesely, M. L., Doskey, P. V., 1993. Numerical Modeling of the Turbulent Diffusion
420 and Chemistry of NO_x, O₃, Isoprene, and Other Reactive Trace Gases in and Above a Forest
421 Canopy. *Journal of Geophysical Research* 98(D10), 18,339–18,353, doi:10.1029/93JD01862.

422 Ganzeveld, L., et al., 2008. Surface and boundary layer exchanges of volatile organic compounds,
423 nitrogen oxides and ozone during the GABRIEL campaign. *Atmospheric Chemistry and*
424 *Physics* 8, 6223–6243.

425 Guenther, A., Karl, T., Harley, P., Wiedinmyer, C., Palmer, P. I., Geron, C., 2006. Estimates of
426 global terrestrial isoprene emissions using MEGAN. *Atmospheric Chemistry and Physics* 6,
427 3181-3210.

428 Grell, G. A., Peckham, S. E., Schmitz, R., McKeen, S. A., Frost, G., Skamarock, W. C., Eder, B.,
429 2005. Fully coupled online chemistry within the WRF model. *Atmospheric Environment* 39,
430 6957–6975.

431 Herwehe, J. A., Otte, T. L., Mathur, R., Rao, S. T., 2011. Diagnostic analysis of ozone
432 concentrations simulated by two regional-scale air quality models. *Atmospheric Environment*
433 45(33), 5957-5969

434 Hu, X.-M., Nielsen-Gammon, J. W., Zhang, F., 2010. Evaluation of Three Planetary Boundary
435 Layer Schemes in the WRF Model. *Journal of Applied Meteorology and Climatology* 49,
436 1831–1844.

437 Hu, X.-M., et al., 2012. Ozone variability in the atmospheric boundary layer in Maryland and its
438 implications for vertical transport model. *Atmospheric Environment* 46, 354-364.

439 Lin, J. T., McElroy, M. B., 2010. Impacts of boundary layer mixing on pollutant vertical profiles
440 in the lower troposphere: Implications to satellite remote sensing. *Atmospheric Environment*
441 44 (14), 1726–1739.

442 Morris, G. A., Ford, B., Rappengluck, B., Thompson, A. M., Mefferd, A., Ngan, F., Lefer, B.,
443 2010. An evaluation of the interaction of morning residual layer and afternoon mixed layer
444 ozone in Houston using ozonesonde data. *Atmospheric Environment* 44, 4024-4034.

445 Neu, U., Kunzle, T., Wanner, H., 1994. On the relation between ozone storage in the residual
446 layer and the daily variation in near surface ozone concentration-A case study. *Boundary-*
447 *Layer Meteorology* 69, 221-247.

448 Nielsen-Gammon, J.W., Hu, X.-M., Zhang, F., Pleim, J.E., 2010. Evaluation of planetary
449 boundary layer scheme sensitivities for the purpose of parameter estimation. *Monthly*
450 *Weather Review* 138, 3400-3417.

451 Noh, Y., Cheon, W. G., Hong, S-Y., Raasch, S., 2003. Improvement of the K-profile model for
452 the planetary boundary layer based on large eddy simulation data. *Boundary-Layer*
453 *Meteorology* 107, 401–427.

454 Poulos, G. S., et al., 2002. CASES-99: A Comprehensive Investigation of the Stable Nocturnal
455 Boundary Layer. *Bulletin of American Meteorological Society* 83, 555–581.

456 Reitebuch, O., Strassburger, A., Emeis, S., Kuttler, W., 2000. Nocturnal secondary ozone
457 concentration maxima analysed by sodar observations and surface measurements.
458 *Atmospheric Environment* 34, 4315-4329.

459 Ryan, W. F., et al., 1998. Pollutant transport during a regional O₃ episode in the Mid-Atlantic
460 states. *Journal of the Air & Waste Management Association* 48, 786–797.

461 Ryan, W. F., 2004. The low-level jet in Maryland: profiler observations and preliminary
462 climatology. A report prepared for the Maryland Department of the Environment.

463 Salmond, J.A., McKendry, I.G., 2002. Secondary ozone maxima in a very stable nocturnal
464 boundary layer: observations from the Lower Fraser Valley, B.C. *Atmospheric Environment*
465 36, 5771–5782.

466 Salmond, J. A., McKendry, I. G., 2005. A review of turbulence in the very stable boundary layer
467 and its implications for air quality. *Progress in Physical Geography* 29, 171–188.

468 Song, J., Liao, K., Coulter, R. L., Lesht, B. M., 2005. Climatology of the Low-Level Jet at the
469 Southern Great Plains Atmospheric Boundary Layer Experiments Site. *Journal of Applied*
470 *Meteorology* 44, 1593–1606.

471 Stockwell, W. R., Kirchner, F., Kuhn, M., Seefeld, S., 1997. A new mechanism for regional
472 atmospheric chemistry modeling. *Journal of Geophysical Research* 102, 25 847–25 879.

473 Sun, J., et al., 2002. Intermittent turbulence associated with a density current passage in the
474 stable boundary layer. *Boundary-Layer Meteorology* 105, 199–219.

475 Sun, J., et al., 2003. Atmospheric disturbances that generate intermittent turbulence in nocturnal
476 boundary layers. *Boundary-Layer Meteorology* 110, 255–279.

477 Stull, R. B., 1988. *An Introduction to Boundary Layer Meteorology*, Kluwer, Norwell, Mass.

478 Talbot, R., Mao, H., Sive, B., 2005. Diurnal characteristics of surface level O₃ and other
479 important trace gases in New England. *Journal of Geophysical Research* 110, D09307,
480 doi:10.1029/2004JD005449.

481 Tjernström, M., Balsley, B. B., Svensson, G., Nappo, C. J., 2009. The Effects of Critical Layers
482 on Residual Layer Turbulence. *Journal of the Atmospheric Sciences* 66, 468–480.

483 Tong, N.Y.O., Leung, D.Y.C., Liu, C.H., 2011. A review on ozone evolution and its relationship
484 with boundary layer characteristics in urban environments. *Water, Air, & Soil Pollution* 214,
485 13-36.

486 Tucker, S. C., et al., 2010. Relationships of coastal nocturnal boundary layer winds and
487 turbulence to Houston ozone concentrations during TexAQS 2006. *Journal of Geophysical*
488 *Research* 115, D10304, doi:10.1029/2009JD013169.

489 Wesely, M. L., 1989. Parameterization of surface resistances to gaseous dry deposition in region-
490 scale numerical models. *Atmospheric Environment* 23, 1293–1304.

491 Wexler, H., 1961. A boundary layer interpretation of the low-level jet. *Tellus*, 13, 368–378.

492 Whiteman, C. D., Bian, X., Zhong, S., 1997. Low-Level Jet Climatology from Enhanced
493 Rawinsonde Observations at a Site in the Southern Great Plains. *Journal of Applied*
494 *Meteorology* 36, 1363–1376.

495 Yorks, J.E., Thompson, A. M., Joseph, E., Miller, S. K., 2009. The Variability of Free
496 Tropospheric Ozone over Beltsville, Maryland (39N, 77W) in the Summers 2004-2007.
497 *Atmospheric Environment* 43, 1827-1838.

498 Zhang, D.-L., Zhang, S., Weaver, S. J., 2006. Low-Level Jets over the Mid-Atlantic States:
499 Warm-Season Climatology and a Case Study. *Journal of Applied Meteorology and*
500 *Climatology* 45, 194–209.

501 Zhang, F., Bei, N., Nielsen-Gammon, J. W., Li, G., Zhang, R., Stuart, A. L., Aksoy, A., 2007.
502 Impacts of meteorological uncertainties on ozone pollution predictability estimated through
503 meteorological and photochemical ensemble forecasts. *Journal of Geophysical*
504 *Research* 230, D04304, doi:10.1029/2006JD007429.

505 Zhang, J., Rao, S. T., 1999. The role of vertical mixing in the temporal evolution of ground-level
506 ozone concentrations. *Journal of Applied Meteorology* 38, 1674 – 1691.

507 Zhang, J., Rao, S. T., Daggupati, S. M., 1998. Meteorological Processes and Ozone
508 Exceedances in the Northeastern United States during the 12–16 July 1995 Episode. *Journal*
509 *of Applied Meteorology*, 37, 776–789.

510 Zhang, Y., Dubey, M. K., Olsen, S. C., Zheng, J., Zhang, R., 2009. Comparisons of WRF/Chem
511 simulations in Mexico City with ground-based RAMA measurements during the 2006-
512 MILAGRO. *Atmospheric Chemistry and Physics*, 9, 3777–3798.

513 Zhong, S., Fast, J. D., Bian, X., 1996. A Case Study of the Great Plains Low-Level Jet Using
514 Wind Profiler Network Data and a High-Resolution Mesoscale Model. *Monthly Weather*
515 *Review* 124, 785–806.